AD NUMBER

AD891216

NEW LIMITATION CHANGE

TO

Approved for public release, distribution unlimited

FROM

Distribution authorized to U.S. Gov't. agencies only; Test and Evaluation; 04 FEB 1972. Other requests shall be referred to Office of Naval Research, ATTN: Code 468, Arlington, VA 22217.

AUTHORITY

ONR ltr dtd 29 Aug 1973

# COMPUTER PROGRAMS FOR UNDERWATER SOUND FIELDS DUE TO AIRBORNE SOURCES

John F. Waters

January 1972

Technical Note Number 144
Contract N00014-70-C-0301



Prepared for
OFFICE OF NAVAL RESEARCH
Code 468
Arlington, Virginia 22217



HYDROSPACE RESEARCH CORPORATION
2150 Fields Road
Rockville, Maryland 20850

# COMPUTER PROGRAMS FOR UNDERWATER SOUND FIELDS DUE TO AIRBORNE SOURCES

John F. Waters

January 1972

Technical Note Number 144
Contract N00014-70-C-0301

Prepared for
OFFICE OF NAVAL RESEARCH
Code 468
Arlington, Virginia 22217

HYDROSPACE RESEARCH CORPORATION
2150 Fields Road
Rockville, Maryland 20850

## SUMMARY

An aircraft flying over water produces a significant underwater sound field in the water directly beneath it. Acoustic ray theory can be used to obtain a useful approximate description of the underwater sound field in terms of sound pressure levels. Details of the theory are presented. Computer programs which implement the theory are documented. The results include time histories of acoustic signal angles of arrival at the underwater receiver; time histories of sound pressure levels received at various depths; and equipressure contour descriptions of the underwater sound field.

TABLE OF CONTENTS

## LIST OF ILLUSTRATIONS

Section 1

# INTRODUCTION

An aircraft flying over water produces a significant underwater sound field in the water directly beneath it.

Given a measurement of the aircraft noise source level in air, acoustic ray theory can be used to obtain a useful approximate description of the underwater sound field in terms of sound pressure levels. The purpose of this note is to document a set of computer programs which have been developed to characterize underwater sound fields produced by airborne point sources under specific circumstances.

Section 2 of this note summarizes the existing acoustic ray theory of sound transmission from air into a body of water. In Section 3, underwater sound fields due to airborne point sources are characterized in general. Section 4 describes the set of computer programs which have been developed. Finally, Section 5 provides comparisons between the predictions of ray theory and experimental measurements, which provide validation of the theory.

# Section 2

# SOUND TRANSMISSION FROM AIR INTO BODY OF WATER

## 2.1 EXISTING ACOUSTIC RAY THEORY

The existing acoustic ray theory of sound transmission from an airborne point source across a flat air-water interface into a body of water has been well established for about 15 years, due to work by Hudimac[1] and Horton.[2]

Consider the general acoustic ray geometry shown in Figure 2-1. There is a stationary point sound source in the air at a height $h_1$ above the flat surface of the water. In a given frequency band the source sound pressure level, $p_0$, is known at some reference distance, $r_0$.

The sound pressure level at a point, R, in the water is to be determined. In the acoustic ray theory description, sound energy is characterized as propagating along a set of sound rays which are emitted radially from the point source, and which are redirected upon crossing the air-water interface. The basic assumption is that sound energy does not cross rays.

Sound pressure level $p_R$ at underwater point R may be determined in three steps. First, the reduction in sound pressure due to spherical divergence as the sound energy propagates along a given ray from the source to the water is determined. Second, the change in sound pressure as the sound energy is transmitted across the air-water interface is determined. Third, the reduction of sound pressure due to geometrical spreading as the sound propagates along a given ray from the interface to the receiver at point R is determined.

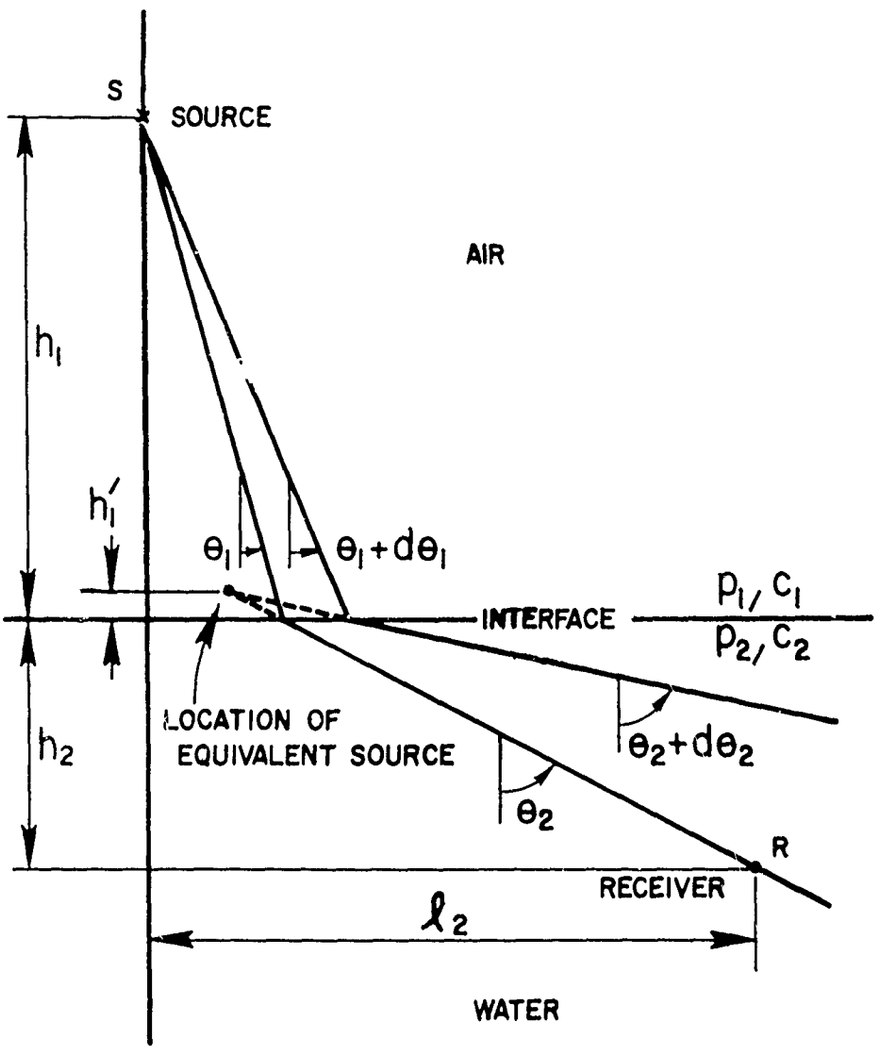


Figure 2-1. Acoustic Ray Geometry for Air-to-Water Sound Transmission

The first reduction in sound intensity which occurs as the acoustic energy propagates through the air is given by

$$I_1 = (r_0^2/r_1^2)\, I_0,$$

where $I_0$ is the source intensity at reference distance $r_0$, and $I_1$ is the sound intensity on the air side of the air-water interface, at a distance $r_1$ from the source, as shown in Figure 2-1. The corresponding sound pressure amplitude is

$$p_1 = (r_0/r_1)\, p_0.$$

The second change in sound intensity as the acoustic energy is transmitted across the air-water interface is a strong function of the acoustic impedances of the air and water, and is also to some extent a function of the angle of incidence of the acoustic energy upon the surface of the water. Two factors are of importance. These are the fraction of the incident acoustic power which is transmitted across the interface, and the change in the cross-sectional area of the ray bundle as it crosses the interface. As derived in detail by Brekhovskikh[3] for the case of plane waves, the relationship between incident sound intensity, $I_1$, and transmitted sound intensity, $I_2$, is given by

$$I_2 = \frac{4\rho_1 c_1 \rho_2 c_2}{(\rho_2 c_2 + B\rho_1 c_1)^2}\ I_1,$$

and the corresponding incident and transmitted sound pressure amplitudes are related by

$$p_2 = \frac{2\rho_2 c_2}{(\rho_2 c_2 + B\rho_1 c_1)}\ p_1,$$

where $\rho_1 c_1$ and $\rho_2 c_2$ are the acoustic impedances of the air and water, respectively, and where $B = \cos\theta_2/\cos\theta_1$.

Angle $\theta_2$ is related to angle $\theta_1$ through Snell's law:

$$\sin \theta_2 = (c_2/c_1) \sin \theta_1.$$

Thus, numerical factor B is a function only of $\theta_1$ and the sound speeds $c_1$ and $c_2$ in air and water, respectively. Snell's law is a consequence of the basic physical boundary condition requirements that the sound pressure amplitude and the normal component of particle velocity are continuous across the air-water interface.

The third reduction in sound intensity as the acoustic energy propagates through the water is given by

$$I_R = \frac{(r_1 \cos\theta_1)^2}{(h_1 + c_2 h_2 / B^3 c_1)\,(h_1 + c_2 h_2 / B c_1)}\, I_2$$

where $I_R$ is the sound intensity at the underwater receiver point R, and where $h_1$ and $h_2$ are the vertical distances shown in Figure 2-1. The corresponding sound pressure amplitude at point R is given by

$$p_R = \frac{\rho_2 c_2 r_1 \cos\theta_1}{(h_1 + c_2 h_2 / B^3 c_1)^{1/2}\,(h_1 + c_2 h_2 / B c_1)^{1/2}}\, p_2.$$

To obtain expressions for the received sound intensities and pressure amplitudes as functions of the corresponding source values and the appropriate physical parameters, the sets of three respective intensity and pressure expressions indicated above are combined. The overall results are:

$$I_R = \frac{\rho_1 c_1 (2 r_0 \cos\theta_1)^2}{(h_1 + c_2 h_2 / B^3 c_1)\,(h_1 + c_2 h_2 / B c_1)} \frac{I_0}{(1 + B \rho_1 c_1 / \rho_2 c_2)^2};$$

$$p_R = \frac{2r_0\cos\theta_1}{(h_1+c_2h_2/B^3c_1)^{1/2}\ (h_1+c_2h_2/Bc_1)^{1/2}} \frac{p_0}{(1+B\rho_1c_1/\rho_2c_2)}.$$

## 2.2 PHYSICAL DESCRIPTION

To aid in the visualization of underwater sound fields due to airborne point sources, a physical interpretation of the abstract mathematical expressions summarized in the previous section is needed.

In the air, there is spherical divergence of sound from the point source. Sound intensity diminishes as the inverse square of distance from the source. Sound pressure amplitude diminishes as the inverse of distance from the source. Thus, both intensity and pressure diminish by 6 dB per distance doubled, and by 20 dB per decade increase in distance from the source.

At the air-water interface, any acoustic energy propagating along a ray which subtends an angle greater than about 13 degrees from the vertical is totally reflected from the surface of the water. As indicated later in Figure 3-5, only acoustic energy within a cone having a half-angle equal to the critical angle of about 13 degrees is transmitted into the water. Even in this region where the critical cone intersects the interface, only a small fraction of the incident acoustic intensity is transmitted. The transmission loss in acoustic intensity is about 29 dB.

However, it is important to note that there is not a corresponding diminution of sound pressure amplitude as a result of crossing the air-water interface. The acoustic impedance of water is much greater than that of air. Thus, an in-phase reflection of the incident sound pressure wave occurs. The total sound pressure amplitude at any instant at a point in the air just above the air-water interface is almost double the instantaneous amplitude of the incident sound pressure wave. Since there is continuity of sound pressure across the air-water

interface, this means there is sound pressure doubling in the water just below the air-water interface as well. Rather than being decreased by 29 dB upon crossing the air-water interface, as is the sound intensity, the sound pressure amplitude is actually increased by 6 dB as the acoustic energy crosses the interface. Thus, the sound pressure levels in the water are about 35 dB higher than the corresponding sound intensity levels in the water.

The above situation is typical for sound transmission from a low impedance medium (air) to a high-impedance medium (water). The acoustic intensity diminishes significantly, while the sound pressure amplitude is essentially unchanged. This is not the case for sound transmission from water to air. The acoustic energy reflected from a water-air interface is out-of-phase with the incident energy. Sound pressure cancellation occurs in the water, rather than pressure doubling. Depending upon the angle of incidence at the water-air interface, the sound intensity diminishes by 29 dB or more and the sound pressure amplitude diminishes by 66 dB or more, as acoustic energy is transmitted from water into air.

Returning now to the case of sound transmission from air to water, after sound crosses the air-water interface, its intensity and pressure amplitude diminish further as it geometrically spreads during propagation through the water. Acoustic energy propagating vertically downward from the airborne source spreads in the water as if it were radiated from a point on the vertical axis, at a height on the vertical axis given by

$$h_1' = \frac{c_1}{c_2} h_1.$$

Acoustic energy entering the water along the critical ray, however, spreads in the vertical plane as if it originated from a source which was at the air-water interface, at the point of intersection of the critical

ray. Thus, most of the acoustic power transmitted across the air-water interface propagates nearly vertically downward. The amount of acoustic energy redirected in near-horizontal directions is relatively small.

## 2.3 SHORTCOMINGS OF EXISTING THEORY

The principal shortcoming of the existing acoustic ray theory of underwater sound due to an airborne point source, as developed by Hudimac and by Horton, is a parametric one. An expression for the received sound intensity or pressure amplitude is available only in terms of the source values and the following physical parameters: source height, $h_1$; receiver depth, $h_2$; sound speeds, $c_1$ and $c_2$; densities, $\rho_1$ and $\rho_2$; and the angle of incidence, $\theta_1$, of the airborne sound upon the air-water interface.

The difficulty is that $\ell_2$, the horizontal displacement of the receiver from a vertical line through the source, is not one of the parameters. In the existing form of the theory, one cannot specify the source-interface-receiver geometry by means of distances $h_1$, $h_2$ and $\ell_2$ and then solve directly for the sound intensity or pressure amplitude at the receiver.

Instead, for a given receiver location, it is necessary to use parameters $h_1$, $h_2$ and $\ell_2$ along with the sound speeds $c_1$ and $c_2$ in Snell's law to determine the angle of incidence, $\theta_1$. This requires the solution of a quartic equation in $\sin^2\theta_1$, so the overall task is not easily accomplished in closed form by hand for many points.

A second shortcoming of the existing theory is the presentation of the results in terms of acoustic intensity only. Sound pressure levels are preferable. In experimental acoustics, sound pressure rather than sound intensity is the practical measurable quantity. In air to water sound transmission, the sound pressure and intensity levels are the same in air, but in the water the pressure levels are about 35 dB higher

than the intensity levels, due to the change in acoustic impedances. This 35 dB difference is significant when underwater sound fields due to airborne noise sources are compared with underwater sound pressure levels due to various underwater sources.

Section 3

# CHARACTERIZATION OF UNDERWATER SOUND FIELD

## 3.1 EQUIPRESSURE CONTOURS

As indicated at the end of Section 2.1, the received underwater sound pressure amplitude due to an airborne source is, according to acoustic ray theory,

$$p_R = \frac{2r_0 \cos \theta_1}{(h_1 + c_2 h_2 / B^3 c_1)^{1/2} \, (h_1 + c_2 h_2 / B c_1)^{1/2}} \frac{p_0}{(1 + B \rho_1 c_1 / \rho_2 c_2)},$$

where

$$B \equiv \frac{\cos \theta_2}{\cos \theta_1} \quad \text{and where}$$

$p_0$ = source sound pressure amplitude at $r_0$;

$r_0$ = reference distance for source amplitude;

$\theta_1$ = angle of ray from source to interface;

$\theta_2$ = angle of ray from interface to receiver;

$h_1$ = source height above interface;

$h_2$ = receiver depth below interface;

$c_1$ = sound speed in air;

$c_2$ = sound speed in water;

$\rho_1$ = density of air;

$\rho_2$ = density of water;

and $p_R$ = received sound pressure amplitude.

For a given sound source and air-water medium, parameters $p_0$, $r_0$, $c_1$, $c_2$, $\rho_1$ and $\rho_2$ have constant values. The three basic distances required to locate an underwater receiver point relative to the sound source are height $h_1$, depth $h_2$, and horizontal offset $\ell_2$, as shown in Figure 3-1. However, while the above expression for $p_R$ involves $h_1$ and $h_2$ directly, it is not an explicit function of $\ell_2$. Distance $\ell_2$ enters only implicitly, through angles $\theta_1$ and $\theta_2$.

To evaluate the above expression for $p_R$ for a given receiver location, that is, for known values of parameters $h_1$, $h_2$ and $\ell_2$, it is necessary to solve for $\theta_1$ and $\theta_2$. This may be done by considering the geometry of Figure 3-1, and by using Snell's law to relate $\theta_2$ to $\theta_1$ through the sound speeds, $c_2$ and $c_1$. For known values of $h_1$, $h_2$ and $\ell_2$, the values of $\theta_1$, $\theta_2$ and $\ell_1$ are unknown. Three equations which can be used to determine the unknowns are, from the figure and from Snell's law,

$$\ell_1 = h_1 \tan \theta_1;$$

$$(\ell_2 - \ell_1) = h_2 \tan \theta_2;$$

$$\sin \theta_2 = (c_2/c_1) \sin \theta_1.$$

The problem of solving the above three equations simultaneously reduces to the problem of solving a quartic algebraic equation in $\sin^2 \theta_1$:

$$a_4 x^4 + a_3 x^3 + a_2 x^2 + a_1 x + a_0 = 0$$

where $x \equiv \sin^2 \theta_1$ and where

$$a_4 = k^4 [\ell_2^4 + (h_1^2 - h_2^2)^2 + 2\ell_2^2 (h_1^2 + h_2^2)];$$

$$a_3 = -2k^2 [(k^2 + 1)\ell_2^4 + h_1^4 + k^2 h_2^4 + (k^2 + 2)\ell_2^2 h_1^2 + (2k^2 + 1)\ell_2^2 h_2^2 - (k^2 + 1) h_1^2 h_2^2];$$

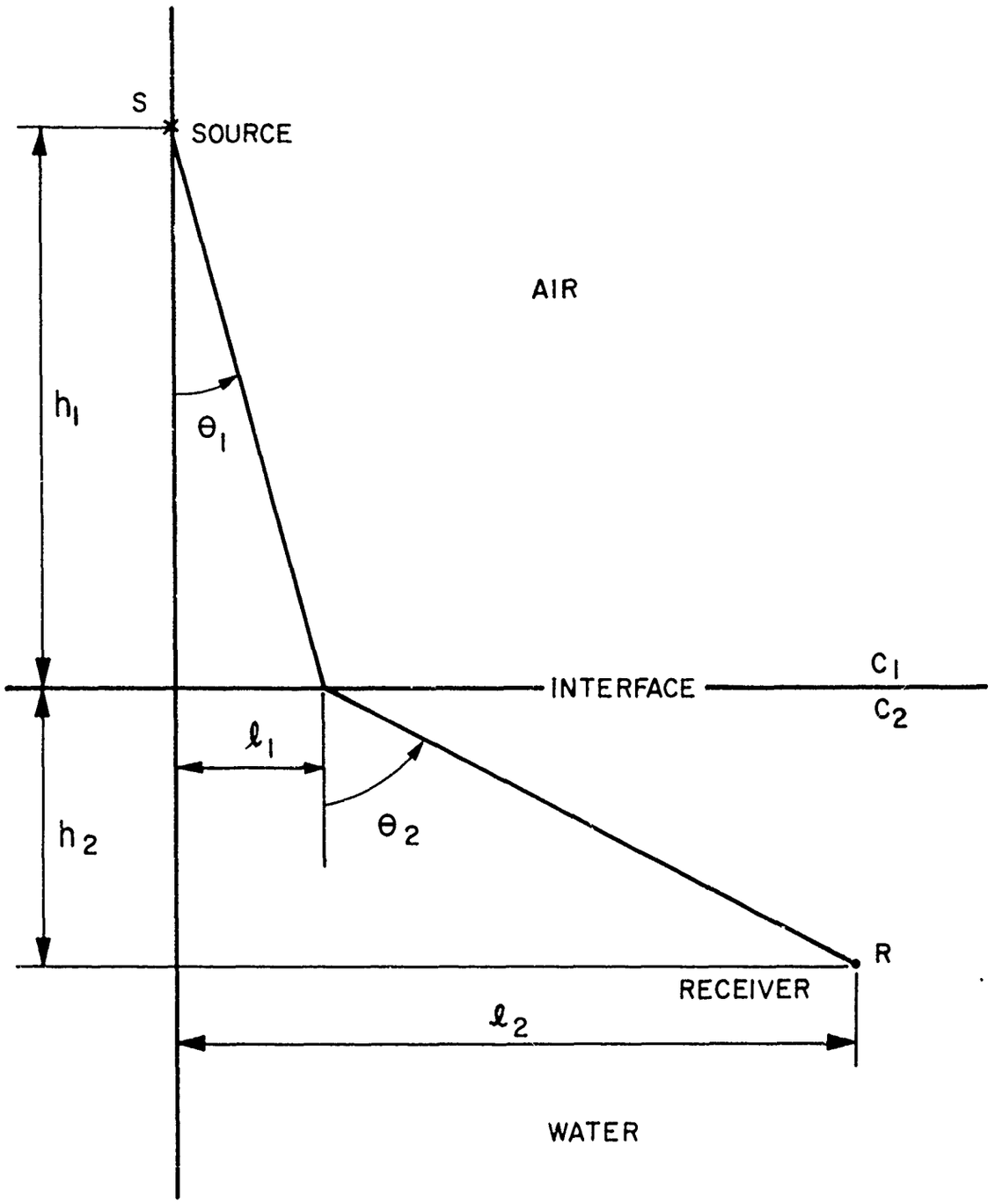


Figure 3-1. Bending of Acoustic Ray at Air-Water Interface

$$a_2 = [(k^4 + 4k^2 + 1)\,\ell_2^4 + h_1^4 + k^4 h_2^4 + 2k^2(2k^2 + 1)\,\ell_2^2 h_1^2 + 2k^2(k^2 + 2)\,\ell_2^2 h_2^2 - 2k^2 h_1^2 h_2^2];$$

$$a_1 = -2[(k^2 + 1)\,\ell_2^4 + \ell_2^2 h_1^2 + k^2 \ell_2^2 h_2^2]; \text{ and}$$

$$a_0 = \ell_2^4,$$

where $k^2 \equiv (c_2/c_1)^2$ in the above.

When a computer is used to calculate the values of $p_R$ at a number of underwater points, the above quartic algebraic equation is easily solved by numerical techniques. Newton's method is used. A first approximation to $\theta_1$, chosen from the range $0 \leq \theta_1 \leq 13$ degrees, is refined iteratively to the desired precision. From this refined value of $\theta_1$, the values of $\theta_2$ and B are calculated. Then $p_R$ is evaluated directly.

The results of evaluating $p_R$ at a number of rectangular grid points serves to determine the underwater sound field, as shown in Figure 3-2. However, a more convenient representation of the underwater sound field is obtained by computing and plotting equipressure contours, as shown in Figure 3-3 for the same sound pressure data presented in Figure 3-2. The equipressure contours are determined by means of interpolation between the sound pressure levels at the rectangular grid points.

The underwater sound field shown in Figures 3-2 and 3-3 is the same as that shown by Horton[2]. The source height is 300 feet. The source sound pressure level is $p_0 = 0$ dB at reference distance $r_0 = 3$ feet. Sound pressure levels are shown in Figures 3-2 and 3-3, whereas Horton shows sound intensity levels, which are about 35 dB lower because of the change in acoustic impedance, as discussed in Section 2.2.

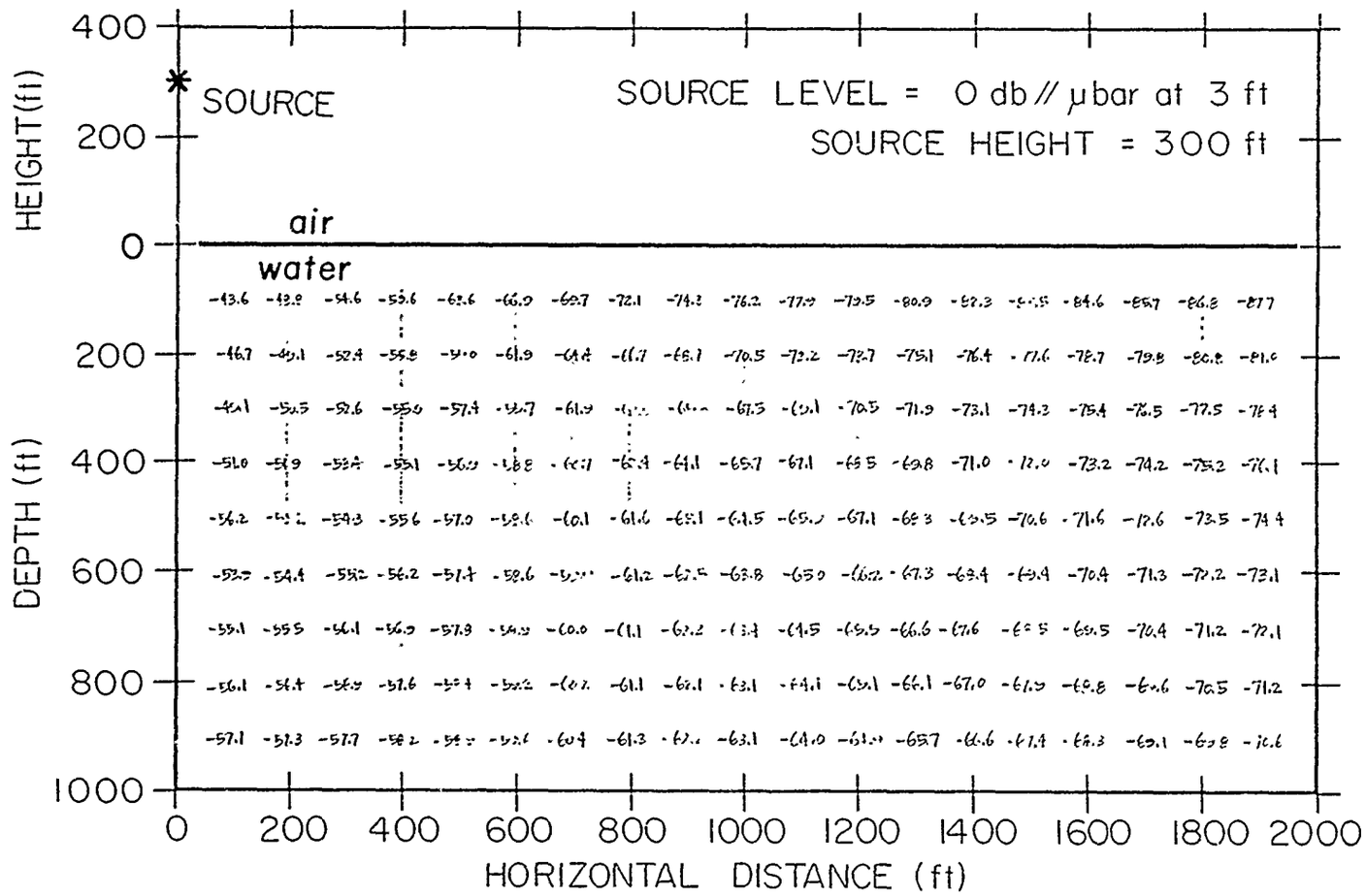


Figure 3-2. Underwater Sound Field due to Airborne Sound Source

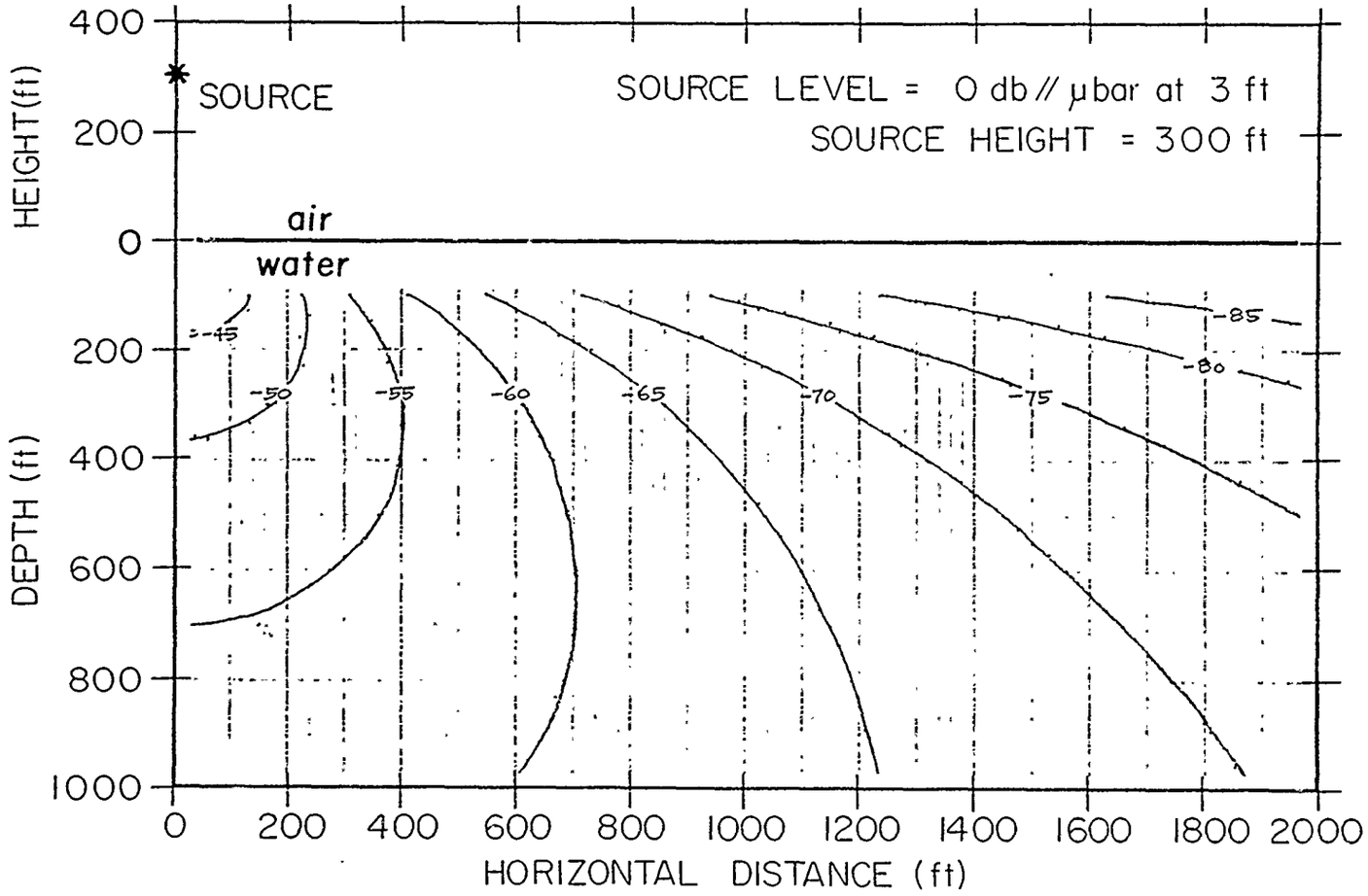


Figure 3-3. Equipressure Contours for Underwater Sound Field due to Airborne Sound Source

## 3.2 SOUND PRESSURE LEVELS VERSUS TIME

The underwater sound field shown in Figures 3-2 and 3-3 has rotational symmetry about the vertical axis through the omnidirectional point source. The figures show vertical slices through the underwater sound field. The vertical axis is at the left, so that horizontal range increases to the right.

In the majority of naval applications of interest, the airborne sound sources are airplanes or helicopters which move horizontally at a high speed relative to the underwater receiver. Time histories of the sound pressure levels at the underwater receiver are useful in these cases. The generation of such time histories may be visualized by moving the underwater sound field shown in Figure 3-3 past an underwater receiver which is located at a fixed depth. Alternatively, the receiver may be visualized as moving through the fixed sound field at a constant depth, at the speed of the relative horizontal motion between the source and receiver. The two concepts are equivalent, except for doppler effects, which have not been considered in the present elementary analysis.

Figure 3-4 shows some typical time histories of received underwater sound pressure levels for a case in which an aircraft flies a straight horizontal path which passes directly over the underwater receiver at time $t = 0$. For this case, the aircraft altitude is 500 feet, rather than 300 feet as for the case shown in Figures 3-2 and 3-3. Sound pressure level time histories are shown for receiver depths of 100, 200, 400 and 800 feet. At the greater depths, the maximum received sound pressure levels diminish, but the time intervals over which the time-varying levels exceed some arbitrary threshold level are increased in duration.

The case in which the aircraft flies directly over the underwater receiver is an extreme example. More often, there will be a horizontal offset between the path of the aircraft and the vertical axis through the array. Time histories of the received sound pressure levels for the case of a nonzero offset

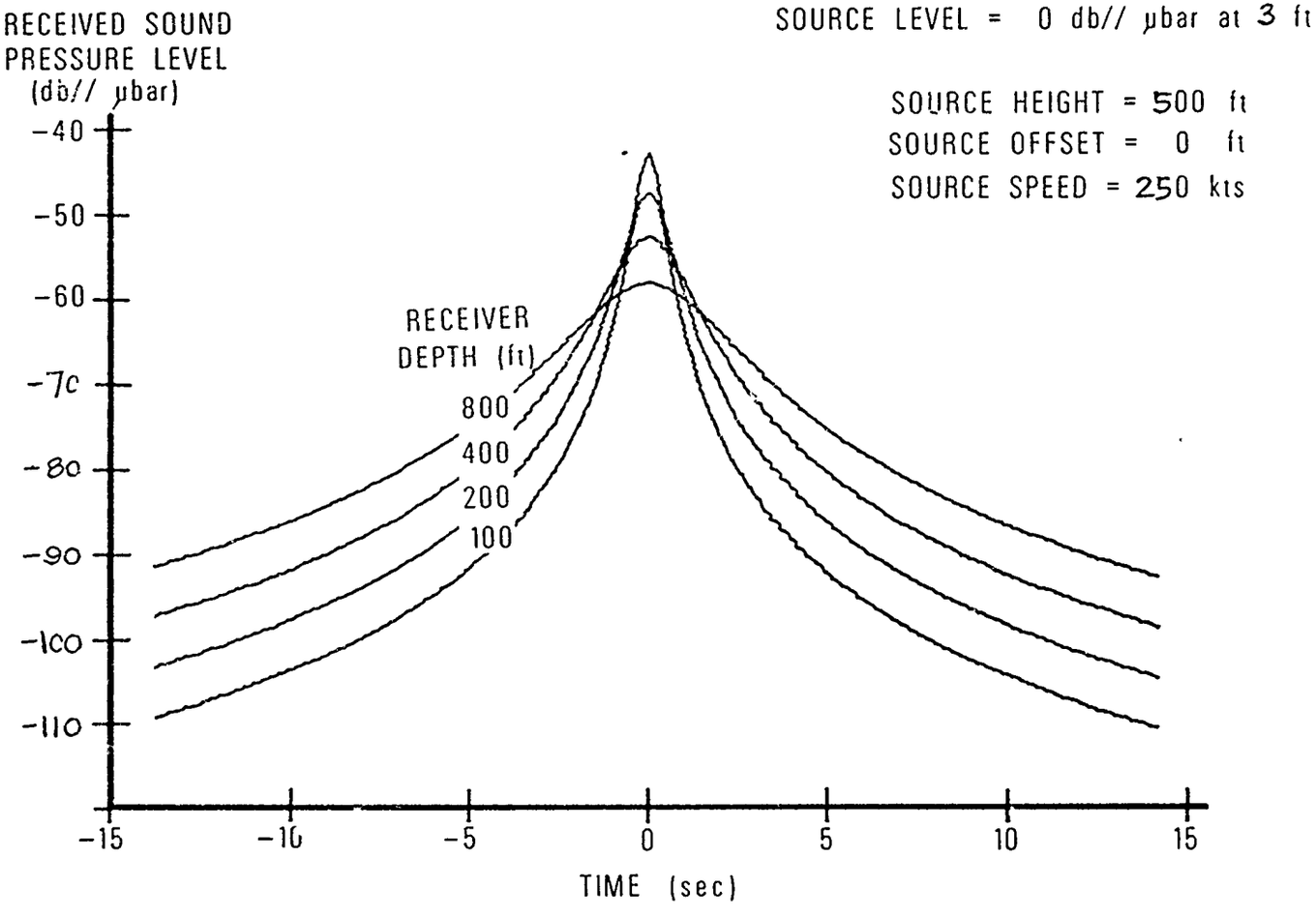


Figure 3-4. Time Histories of Received Underwater Sound Pressure Levels due to Flyover of Airborne Sound Source

of the source are just as easily calculated as for the case of zero offset. However, to visualize the generation of the time histories of received sound pressure levels in the case of nonzero offset, it is necessary to consider the three-dimensional underwater sound field rather than a two-dimensional vertical radial slice through it.

## 3.3 INCLUSION OF RECEIVER NOISE EFFECTS

In most of the applications of interest, the relationship between the transmitted underwater noise signal of the aircraft and the self-noise of the underwater receiver is crucial. Generally, the total signal-plus-noise output from the receiver will be frequency band-limited, so as to concentrate on spectral regions where the aircraft radiated noise signal is strong. Then, two parameters are significant. These are the peak signal-plus-noise to noise ratio, and the duration of the time interval over which the signal-plus-noise level exceeds the noise level by some preselected amount, such as 3 dB.

The self-noise of the receiver may be flow noise, in the case of hull-mounted or towed underwater receivers, or it may be the ambient ocean noise in the frequency band of interest. In either case, it may be safely assumed that the noise adds to the aircraft signal incoherently. This means that the noise and signal powers are added before conversion to decibels. The results are signal-plus-noise level time histories which are similar to those shown in Figure 3-4, but which are limited at their lower bounds by the constant noise level which has been chosen.

## 3.4 GEOMETRY OF ACOUSTIC WAVEFRONTS

The geometry of the acoustic wavefronts involved in the generation of an underwater sound field by an airborne point source is shown in Figure 3-5. This diagram was constructed using only acoustic ray theory.

In the diagram, acoustic rays are shown as straight-line segments, uniformly distributed at 5-degree increments in the water. Snell's law was

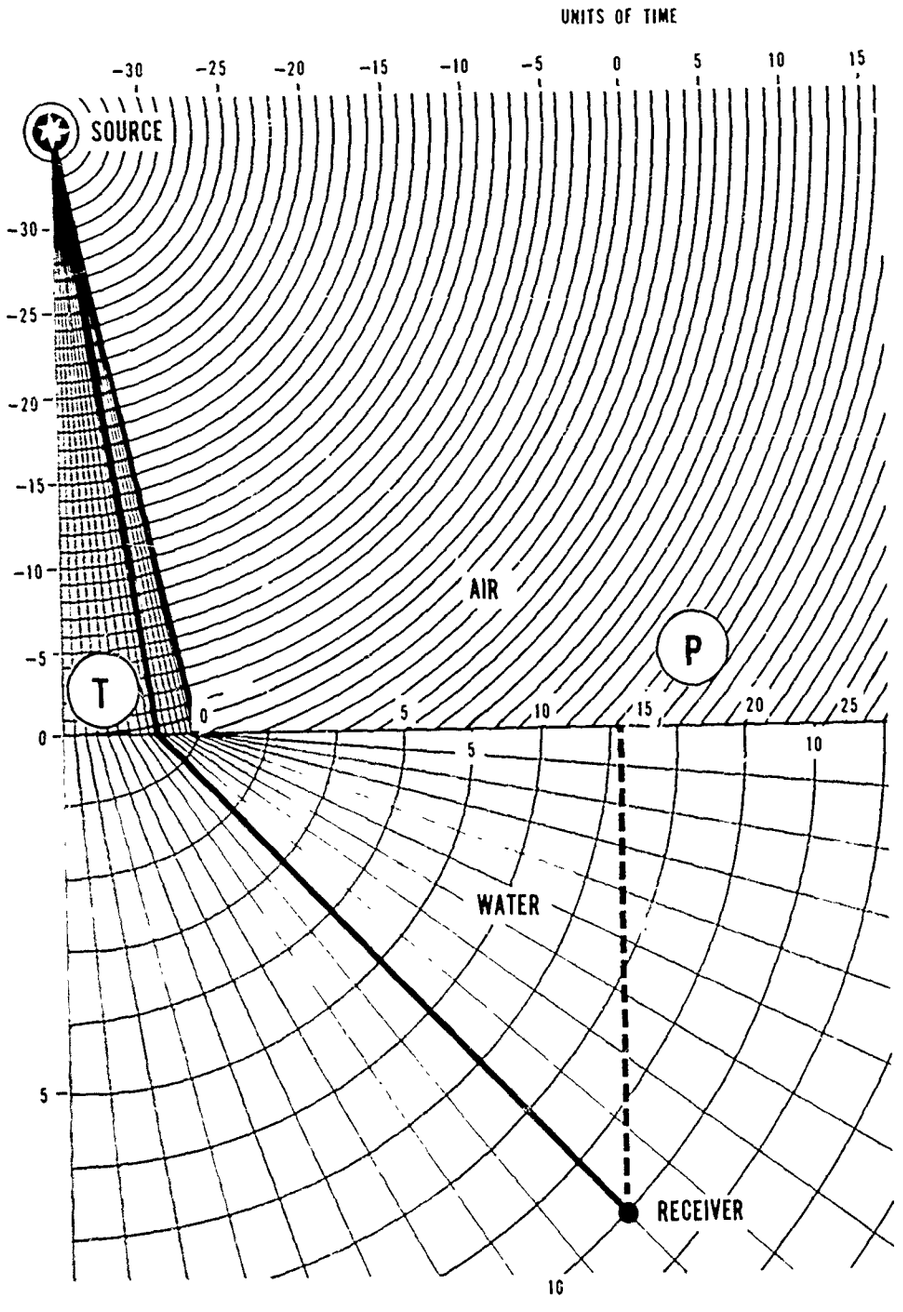


Figure 3-5. Geometry of Acoustic Wavefronts for Underwater Sound Field Due to Airborne Point Source

used to determine the bending of the rays at the air-water interface. Those rays along which sound is transmitted from the air into the water are enclosed in a vertical cone, the half-angle of which is approximately 13 degrees. The region of sound transmission is indicated in the diagram by an encircled "T." As discussed in an earlier section, most of the incident sound energy inside the cone of transmission is reflected back upward at the air-water interface, and yet the sound pressure amplitude (not energy or intensity) transmitted across the interface is appreciable, comparable in magnitude to the incident sound pressure amplitude.

Outside the cone of transmission, the acoustic energy incident upon the air-water interface is totally reflected. Only a slight penetration[3] of sound into the water occurs. This penetrating sound dies out exponentially with depth and with frequency; this is not a sound propagation effect. The region of sound penetration is indicated in the diagram by an encircled "P."

Acoustic wavefronts are shown in Figure 3-5 as curved segments which are perpendicular to the rays. The wavefronts are shown at equally-spaced successive instants of time. One unit of time is the interval between the time at which the spherically spreading airborne acoustic wavefront first reaches the water directly below the source, and the time at which the wavefront impinges upon the water at the critical angle of approximately 13 degrees. This duration is directly proportional to the height of the source above the water. For any source height, as shown in the diagram it requires about 35.5 such intervals of time for sound to propagate from the source to the water directly below. Thus, one unit of time, $\Delta t$, in Figure 3-5 is given approximately by

$$\Delta t = \frac{1}{35.5} \frac{h_1}{c_1},$$

where $h_1$ is the source height and $c_1$ is the speed of sound in air.

## 3.5 ANGLE OF ARRIVAL OF SIGNAL AT RECEIVER

As in Section 3.1, let the position of the underwater receiver relative to the airborne source be described in terms of source height $h_1$, receiver depth $h_2$, and horizontal offset $\ell_2$. Then, as described earlier, a quartic algebraic equation in $\sin^2 \theta_1$ can be solved to determine $\theta_1$, the polar angle of arrival of the signal at the underwater receiver. This is an angle measured relative to a vertical axis through the receiver.

Usually, the underwater receiver has a definite horizontal axis of symmetry. This axis will have a certain azimuthal heading, relative to the heading along which the airborne sound source moves. The angle of arrival of the acoustic signal relative to the horizontal axis of the receiver can then be determined from the polar angle, $\theta_1$, and the relative heading, $\beta$, of the receiver, by consideration of the solid geometry which is involved.

Specifically, suppose that the underwater receiver is a horizontal line array of hydrophones. The axis of symmetry of this receiver is the horizontal line along which the hydrophones lie. With such an array, it is possible to measure only the angle of arrival of an acoustic signal relative to the axis of the array. It is not possible to measure the vertical angle of arrival of the signal at the array.

As a convention, let the heading of the underwater receiver relative to the flight path of the aircraft be zero when the direction of the axis of the receiver is parallel and opposite to the direction of flight of the aircraft. With this convention, when the flight path passes directly over the receiver, with the receiver heading zero degrees, the angle of arrival of the acoustic signal relative to the axis of the array, $\theta_A$, varies from an initial value of zero to a final value of 180 degrees. Similarly, when the receiver heading is 90 degrees, measured either clockwise or counterclockwise from zero, $\theta_A$ = 90 degrees throughout the run, when the flight path passes directly over the receiver.

Figure 3-6 shows time histories of $\theta_A$ for a flight passing directly over the receiver. The source height is 500 feet, the same as in Figure 3-4 where sound pressure level time histories were shown. The receiver depth in Figure 3-6 is 400 feet. Results shown in the figure are consistent with the preceding discussion.

Figure 3-7 shows similar angles of arrival for a source height of 4000 feet. As would be expected on the basis of the acoustic ray geometry shown in Figure 3-5, when the source is at a greater altitude the entire underwater sound field pattern scales up proportionally larger. At a depth of 400 feet, the angles of arrival vary more slowly with time, for the same aircraft speed.

A more interesting case is shown in Figure 3-8. Here, the conditions are the same as for Figure 3-6, except that the flight path does not pass directly over the underwater receiver. The horizontal offset of the flight path from the vertical axis through the receiver is 2000 feet at the closest point of approach. As a result, the time histories of angles of arrival of the signal in Figure 3-8 are somewhat altered from those in Figure 3-6. The angle of arrival is not constant for any receiver heading, when there is a nonzero offset of the flight path. This case is typical. The case of a flight directly over the underwater receiver is an extreme example.

## 3.6 LIMITING CASES FOR UNDERWATER SOUND FIELD

As summarized in detail at the start of Section 3.1, the acoustic ray theory expression for the received sound pressure amplitude due to an airborne point source is

$$p_R = \frac{2r_0 \cos \theta_1}{(h_1 + c_2 h_2/B^3 c_1)^{1/2} (h_1 + c_2 h_2/Bc_1)^{1/2}} \frac{p_0}{(1 + B\rho_1 c_1/\rho_2 c_2)},$$

in which $B = \cos \theta_2/\cos \theta_1$ and where the other parameters are defined in Section 3.1. This expression has been used in the computer programs described in this note.

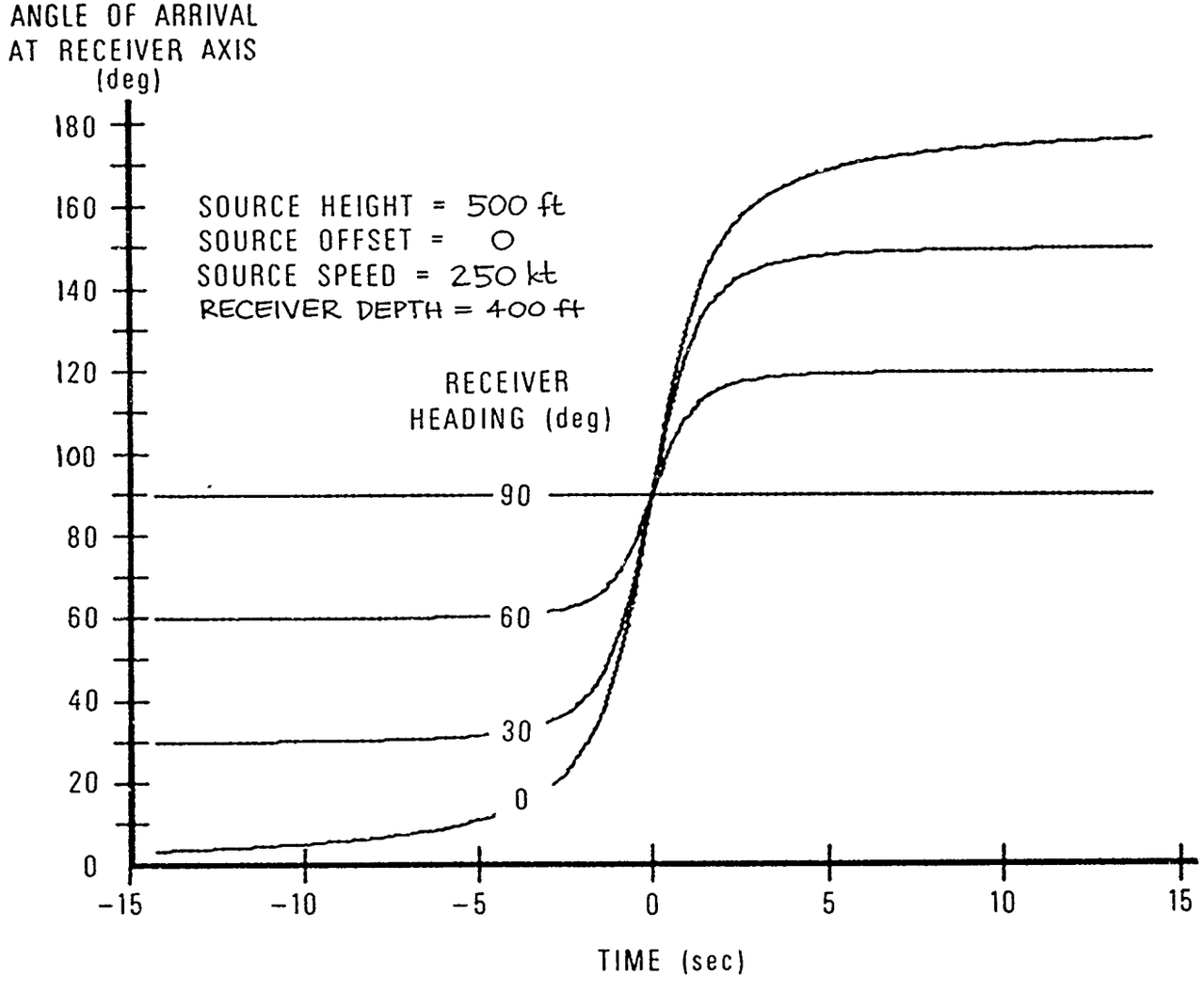


Figure 3-6. Time Histories of Angles of Arrival of Signal at Underwater Receiver Due to Flyover of Airborne Sound Source

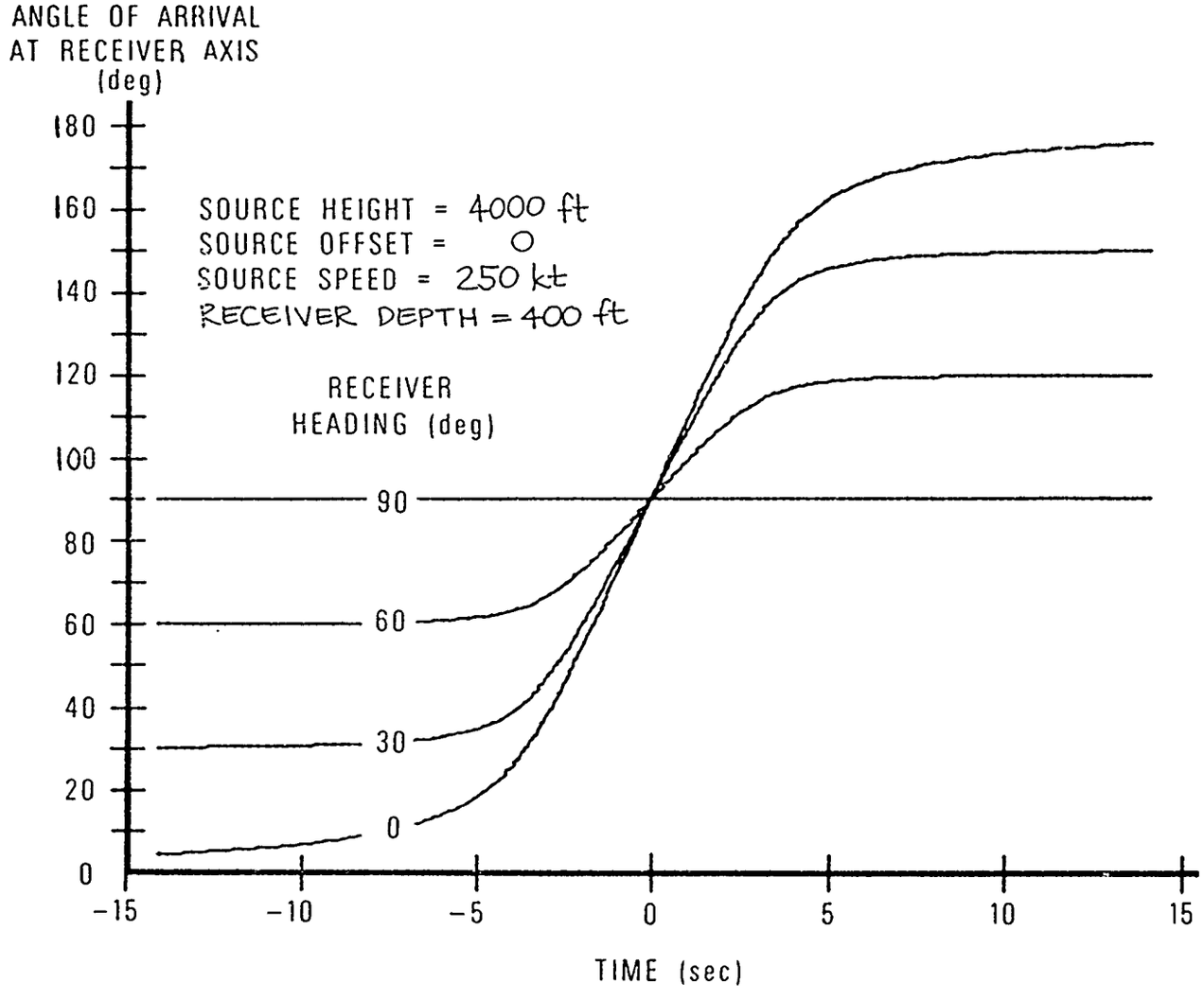


Figure 3-7. Time Histories of Angles of Arrival of Signal at Underwater Receiver due to Flyover of Airborne Sound Source

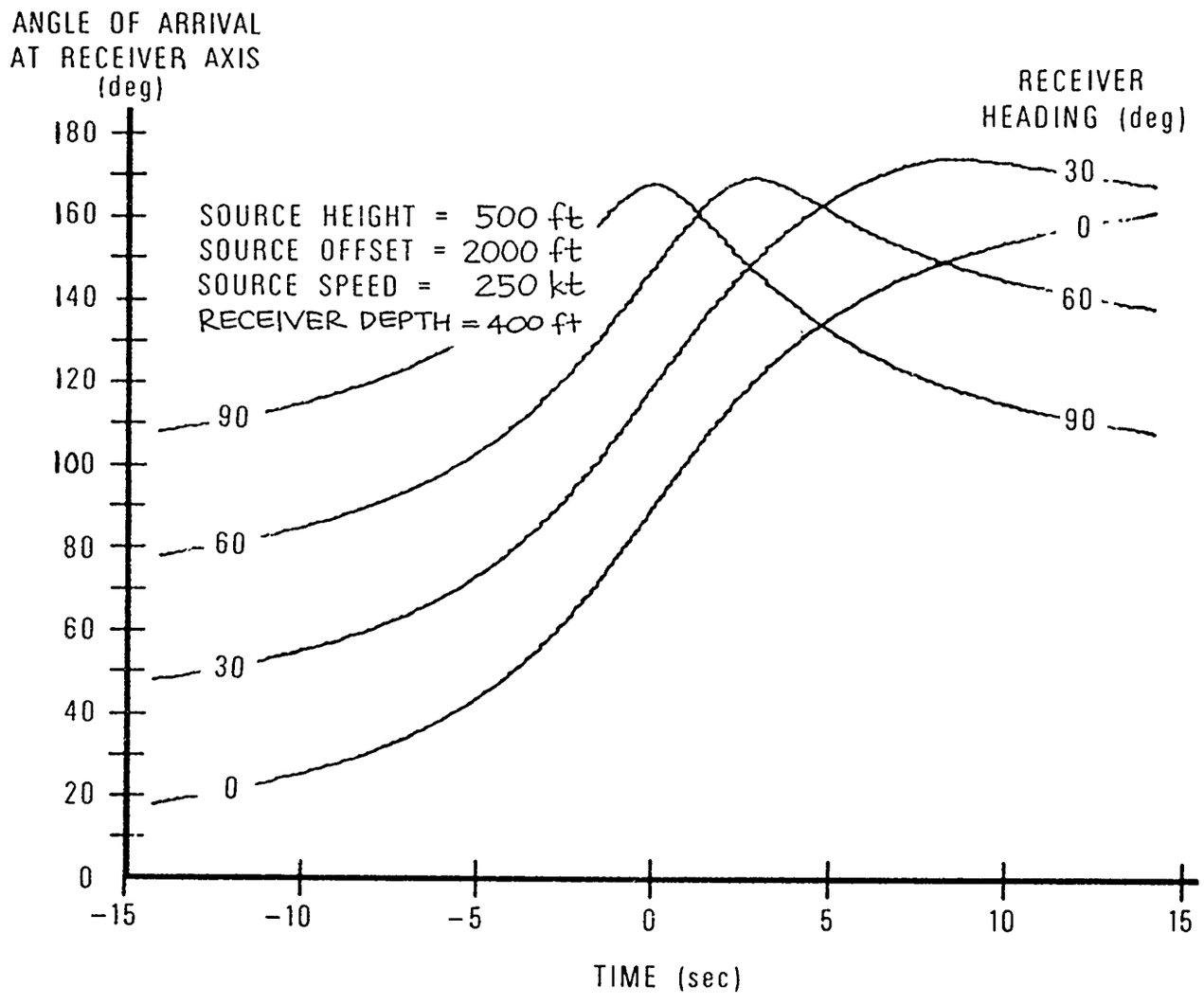


Figure 3-8. Time Histories of Angles of Arrival of Signal at Underwater Receiver due to Flyover of Airborne Sound Source

Consider now some basic physical approximations in the preceding equation. Within the cone of transmission, the angle $\theta_1$ takes on values $0 \leqq \theta_1 \leqq 13$ degrees. Correspondingly, $\cos \theta_1$ takes on values $1 \geqq \cos \theta_1 \geqq 0.97$, so for all practical purposes $\cos \theta_1$ may be approximated as unity, and $B = \cos \theta_2$ is a good approximation. Thus, dimensionless factor B takes on values $0 < B \leqq 1$.

Also, for air and water the ratio $\rho_1 c_1 / \rho_2 c_2$ has a value of about 0.0003. Thus, the approximation $(1 + B\rho_1 c_1 / \rho_2 c_2) = 1$ is a good one.

Using the latter approximation, and with the range of values of B in mind, a good approximation to $p_R$ is the expression

$$p_R = \frac{2B^2 r_0 p_0}{(B^3 h_1 + c_2 h_2 / c_1)^{1/2} \; (Bh_1 + c_2 h_2 / c_1)^{1/2}}.$$

This approximation is valid for all permissible values of $p_0$, $r_0$, $h_1$, $h_2$ and B.

For the first limiting case, consider the situation where the receiver is located directly under the source. In this case, $\theta_1 = 0$, $\theta_2 = 0$, and $B = 1$. The sound pressure amplitude received in the water directly below the source is

$$p_R = \frac{2 r_0 p_0}{(h_1 + c_2 h_2 / c_1)} = \frac{2 r_0 p_0}{(h_1 + 5 h_2)},$$

since the ratio $c_2 / c_1$ is approximately 5 for water to air.

If the receiver depth is small compared with the source height, that is, if $h_2 \leqq h_1/50$, then the received sound pressure amplitude is a function of the source height, $h_1$, only:

$$p_R = 2 \frac{r_0}{h_1} p_0 \quad \text{when} \quad h_2 \leqq h_1/50.$$

This sound pressure amplitude just under the surface of the water, directly below the sound source, is twice the amplitude in the air just above the surface of the water, due to pressure doubling at the interface.

If the receiver depth is greater than double the source height, then the received sound pressure amplitude is a function of the receiver depth, $h_2$, only:

$$p_R = 0.4 \frac{r_0}{h_2} p_0 \quad \text{when} \quad h_2 \geq 2h_1.$$

So long as the receiver depth is greater than double the source height, the underwater sound field pressure levels diminish by 6 dB per depth doubled, directly below the sound source.

Thus, directly under the sound source, the sound pressure levels just under the surface of the water are constant (at double the value in the air just above the surface of the water) down to a depth of roughly $h_2 = h_1/50$. The sound pressure levels then diminish with increasing depth, at a rate which increases with depth from only a fraction of one dB per distance doubled at the depth $h_2 = h_1/50$, to a rate of 6 dB per distance doubled at the depth $h_2 = 2h_1$. At depths greater than $h_2 = 2h_1$, directly under the sound source, the sound pressure levels diminish with depth at a constant rate of 6 dB per distance doubled.

For the second and more general limiting case, consider situations in which the receiver is located far from the source, in units of source height. Referring to the earlier Figure 3-1, let $r_2$ be the slant distance from the point where the acoustic ray crosses the air-water interface, to the point where the receiver is located. That is, let $r_2 = h_2/\cos \theta_2$. If this distance $r_2$ is greater than double the source height, then the expression for the received sound pressure amplitude, $p_R$, can be simplified.

This can be seen by consideration of the case in which $Bh_1 << c_2h_2/c_1$. If this condition is satisfied, then the condition $B^3h_1 << c_2h_2/c_1$ is also satisfied, since $0 < B \leq 1$, and the received sound pressure amplitude becomes

$$p_R = \frac{2B^2r_0p_0}{c_2h_2/c_1} = 0.4B^2\frac{r_0}{h_2}p_0,$$

where $c_2/c_1 = 5$ is assumed.

Since $B = \cos\theta_2 = h_2/r_2$, the received sound pressure amplitude for this case becomes

$$p_R = 0.4\frac{r_0h_2}{r_2^2}p_0.$$

The condition under which the above expression is valid is $Bh_1 << c_2h_2/c_1$, or approximately $r_2 \geq 2h_1$. That is, when the slant distance $r_2$ from the surface below the source to the receiver is greater than double the source height, $h_1$, the above expression is valid. The above expression indicates that at distances $r_2 \geq 2h_1$, the received sound pressure level at a given depth, $h_2$, diminishes at the rate of 12 dB per distance ($r_2$) doubled.

Directly below the sound source, $r_2 = h_2$, and the above expression for $p_R$ at $r_2 \geq 2h_1$ becomes

$$p_R = 0.4\frac{r_0}{h_2}p_0.$$

This agrees with the result obtained previously, for the case directly below the source, at a depth $h_2 \geq 2h_1$.

In general, it can be shown that the equipressure contours which describe the underwater sound field due to an airborne point source take the limiting form of circles, in the more distant regions where $r_2 \geq 2h_1$. The

circles are all tangent to the surface of the water, directly below the sound source. The radii of the circles are easily determined from the values

$$p_R = 0.4 \frac{r_0}{h_2} p_0$$

of the sound pressure amplitudes on the vertical axis passing through the source.

Figure 3-9 is an example of an actually computed underwater sound field in the limiting case in which the airborne sound source is close to the surface of the water. The equipressure contours are clearly circles which are tangent at the air-water interface, directly below the source. In this case, the source was assumed to be a 6-grain dynamite cap which was exploded at a height of one foot above the water. The purpose of computing this particular underwater sound field was to investigate the possibility of using near-surface airborne explosive charges as underwater transient sound sources. Such a technique could avoid surface reflections, bubble pulses and fish kills, all of which are problems with underwater explosions. Also, this technique could direct the sound downward and would limit the amplitude of the horizontally propagating portion of the sound.

The expressions obtained in the above limiting cases are useful in making approximate calculations of underwater sound fields due to airborne sources. However, the exact expressions, such as that for $p_R$ given at the beginning of this section, have always been used in the sequence of computer programs described in this note.

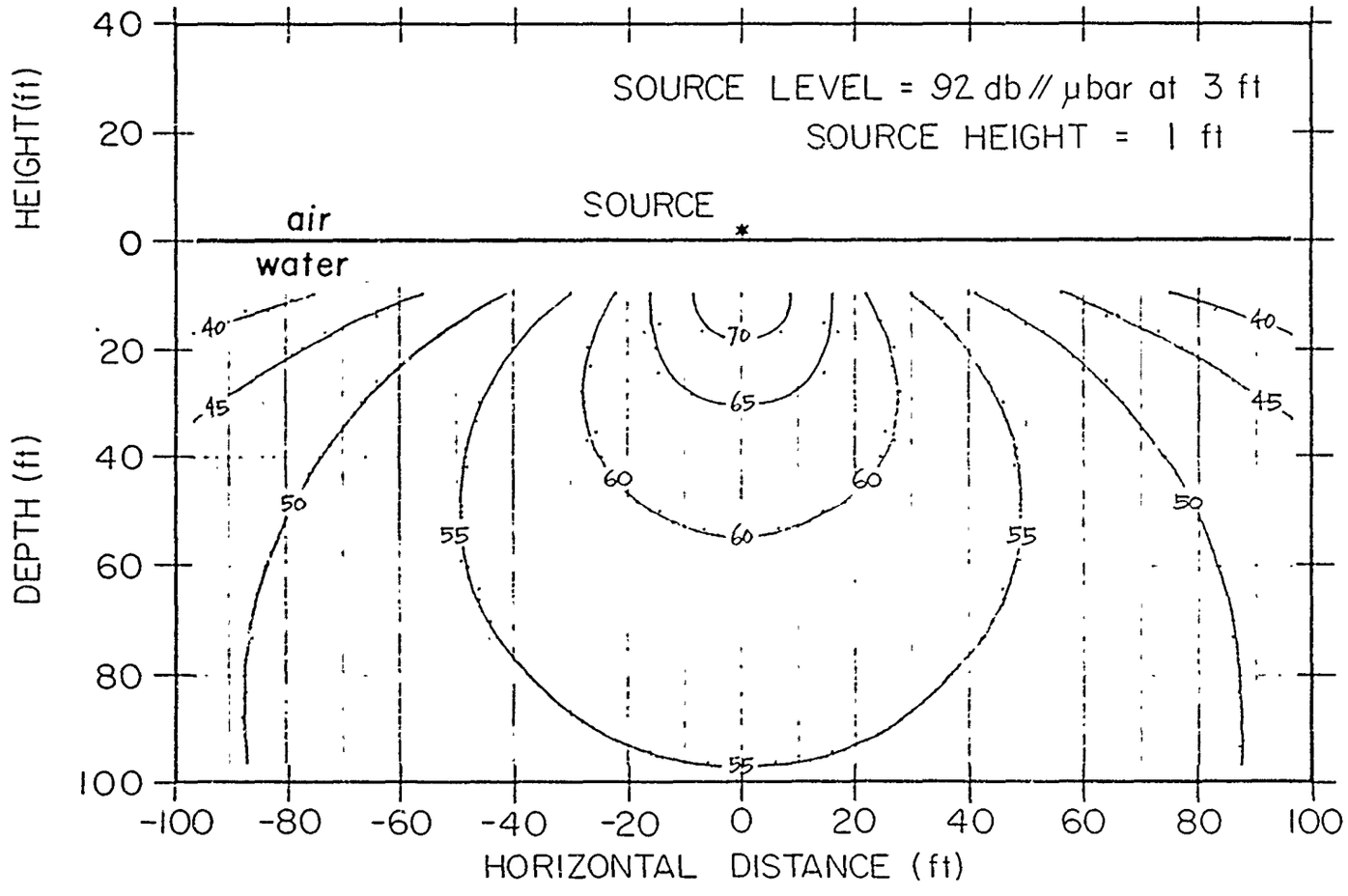


Figure 3-9. Equipressure Contours for Underwater Sound Field due to Airborne Sound Source

Section 4

# SEQUENCE OF COMPUTER PROGRAMS

A sequence of seven computer programs has been developed to compute and machine plot various functions associated with underwater sound fields generated by airborne point sources. The programs have been written in Super Basic for use on a time-sharing computer terminal.

Detailed listings of the seven computer programs are given in Appendix A. The purpose of the present section is to describe the programs from the user's point of view.

Program USF (Underwater Sound Field) is the basic program in the sequence. It is used to compute received sound pressure levels in the water at points on a rectangular grid, as shown previously in Figure 3-2. Vertical angles of arrival of the signal at the various points on the grid are determined as a part of the computation. Computed sets of values are outputted in data files, ready for input into successive programs.

Program AA (Angle of Arrival) is used to compute time histories of angles of arrival, $\theta_A$, of the signal relative to the horizontal axis of the receiver, for various receiver depths and headings. The values of the angles are outputted to a succeeding program, APLOT, for machine plotting of the results. Typical results have been shown in Figure 3-6, 3-7 and 3-8.

Program ADDAMB (Add Ambient) makes possible the inclusion of ambient noise levels in the underwater sound field data computed in

program USF. The ambient noise level which is selected is combined with the noise levels due to the airborne source in a sound power addition, prior to decibel conversion.

Program LPLOT (Levels Plot) is used to prepare time histories of received sound pressure levels at various depths, from program USF, modified by inclusion of the ambient, for machine plotting. Typical results have been shown in Figure 3-4.

Finally, program CON (Contours) is used to compute underwater sound field equipressure contours from the sound field data from program USF, modified by the inclusion of the ambient. An interpolative process is used. The output from CON is prepared for machine plotting by program CPLOT. Typical results have been shown in Figure 3-3.

The three plotting programs, APLOT, CPLOT and LPLOT, are used to properly scale the data, assign the plot origin, and to carry out other similar functions in preparing the data for machine plotting. The data to be plotted is outputted from data files on paper tape at the time-sharing computer terminal. It is then inputted to a minicomputer system which is operated in-house at Hydrospace, for machine plotting on a digital incremental plotter. As the final step in plot preparation, machine plots of data are pasted onto preprinted sheets having the appropriate ordinate and abscissa scales.

The flow diagram for the sequence of seven computer programs is shown in Figure 4-1. The input parameters are different for the various programs; the input parameters for each program are shown in Tables 4-1 and 4-2. The input and output data files for each of the seven programs are summarized in Table 4-3.

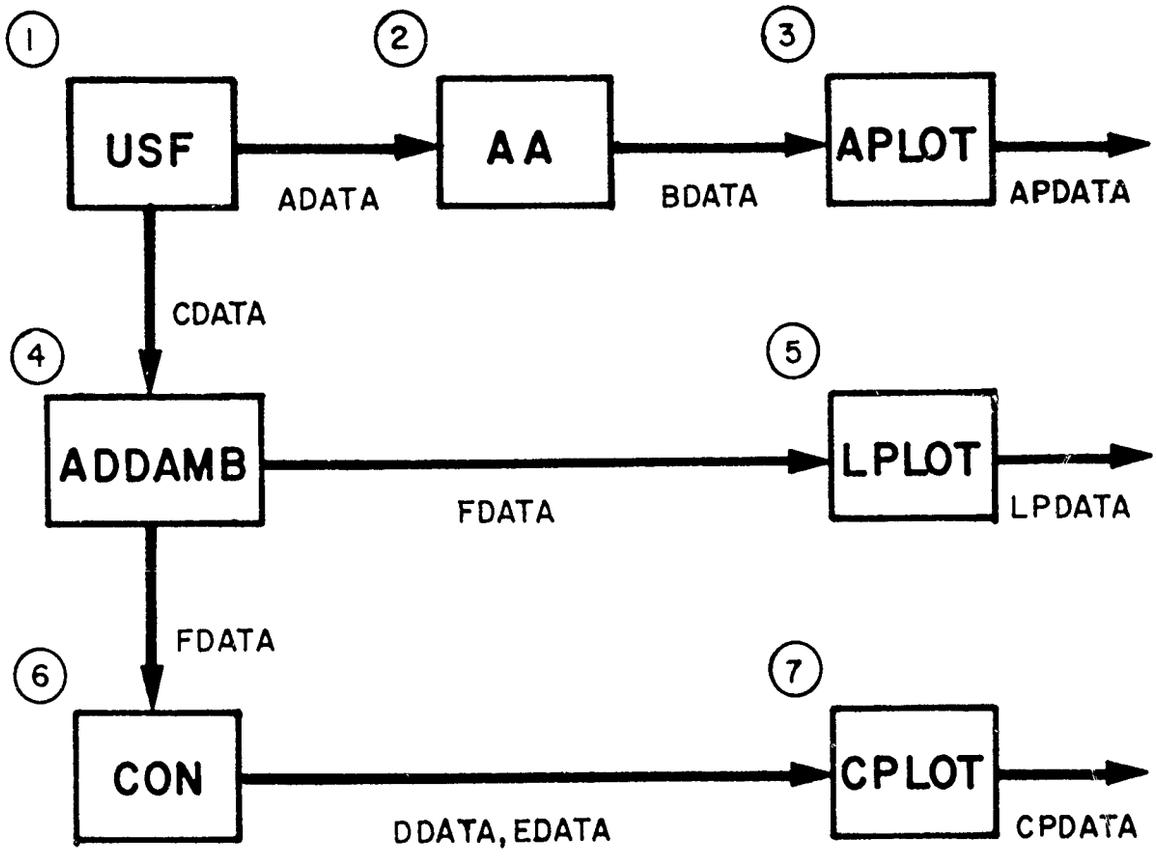


Figure 4-1. Flow Diagram for Sequence of Computer Programs

Table 4-1. Input Parameters

| Parameter | Units | Description |
|---|---|---|
| P1 | dB // $_{\mu}$ bar | Source pressure level in air at distance R1 |
| R1 | ft | Reference distance at which P1 is measured |
| H1 | ft | Height of source above water |
| D1 | ft | Horizontal offset distance from source to vertical axis through receiver at closest point of approach of aircraft flight path |
| U | ft | Grid increment for rectangular grid of points at which underwater sound field is determined |
| Y | ft | Maximum horizontal distance to which underwater sound field is determined in Program USF |
| S1 | knots | Speed of aircraft |
| PO | dB // $_{\mu}$ bar | Ambient sound pressure level |
| Y2 | ft | Maximum horizontal distance to which equipressure contours are to be determined in Program CON |
| C2 | dB | Interval between equipressure contours of underwater sound field in Program CON |
| C1 | dB | Interval between equipressure contours of airborne sound field in Program CPLOT |

Table 4-2. Parameters Inputted to Each Program

| Program | Input Parameters |
|---|---|
| USF | Pi, R1, Hi, D1, U, Y |
| AA | (none) |
| APLOT | S1 |
| ADDAMB | PO |
| LPLOT | S1 |
| CON | Y2, C2 |
| CPLOT | C1 |

Table 4-3. Input and Output Data Files

| Program | Input Data Files | Output Data Files |
|---|---|---|
| USF | (none) | ADATA<br>CDATA<br>UYDATA |
| AA | UYDATA<br>ADATA | BDATA |
| APLOT | UYDATA<br>BDATA | APDATA |
| ADDAMB | UYDATA<br>CDATA | UYDATA<br>FDATA |
| LPLOT | UYDATA<br>FDATA | LPDATA |
| CON | UYDATA<br>FDATA | UYDATA<br>EDATA<br>DDATA |
| CPLOT | UYDATA<br>DDATA<br>EDATA | CPDATA |

It is anticipated that the foregoing rather brief description will suffice as an introduction to the use of the sequence of seven computer programs for the determination of underwater sound fields due to airborne sources. Each of the computer programs is extensively self-explanatory. Upon execution, each program poses to the user a series of questions, such as, "What is the source pressure level, P1, in dB // $_{\mu}$bar at R1?". These questions assure the efficient and error-free inputting of the input variables. The best way of gaining further familiarity with the sequence of computer programs is to put them to actual use.

## Section 5

## COMPARISON BETWEEN RAY THEORY PREDICTIONS AND EXPERIMENTAL MEASUREMENTS

This report has described a sequence of computer programs which implement the acoustic ray theory predictions developed by Hudimac[1] and by Horton[2] for underwater sound fields due to airborne sources.

As indicated by Hudimac[1], the ray theory in this case will not be valid for large horizontal separations ($\ell_2$) of the source and receiver, especially when the receiver is near the surface. That is, the ray theory predictions may be inaccurate when the receiver is located within an acoustic wavelength of the surface, at the source frequency of interest. In these cases, acoustic wave theory rather than ray theory should be applied.

However, the validity of the acoustic ray theory predictions of the underwater sound field directly beneath the aircraft has also been questioned in recent years by Weinstein and Henney[4]. In this work, the zero-frequency limit of the wave theory expression for the underwater sound field directly beneath the aircraft was taken, and it did not agree with the corresponding ray theory expression.

Young[5] has recently made some experimental acoustic measurements to determine which is valid, Hudimac's ray theory or Weinstein's limiting form of wave theory, for the prediction of sound pressure levels at points in the water directly below an airborne point source. It has been concluded that ray theory provides an adequate description in this case, and the limiting form of the wave theory does not. It appears that the zero-frequency limit is too much of an extreme case to apply to noise at useful frequencies, above 10 Hz.

A further comparison between ray theory predictions and experimental measurements has been made recently at Hydrospace, using data from a sonic boom simulation experiment[6] in which the penetration of airborne shock wave energy into a body of water was the principal subject of investigation. (Here, the phenomenon of penetration of an acoustic disturbance across the air-water interface, in the form of a non-propagating evanescent wave accompanying a totally-reflected airborne wave, is distinguished from the phenomenon of transmission of sound across the air-water interface.) In this work, dynamite caps were exploded over a flooded quarry. Transmission effects were measured, in addition to penetration effects.

Figure 5-1 shows the comparison between the experimental measurements and the predictions of ray theory, as determined using the sequence of computer programs described in this note. The experimental values are enclosed with rectangles and are plotted at the points of measurement. The theoretical values are enclosed with ovals and are shown as equipressure contours of the underwater sound field. The source height was 30 ft.

Agreement between the experimental measurements and the predictions of ray theory as shown in Figure 5-1 is quite good, within $\pm$ 3 db in most cases throughout the region shown. This good agreement further validates acoustic ray theory for the prediction of underwater sound fields due to airborne point sources. The investigator who uses the sequence of computer programs described in this note to predict underwater sound fields, given the altitude and source level of the airborne noise source, can do so with confidence that the predictions will be accurate except at points which are very distant horizontally, especially close to the air-water interface.

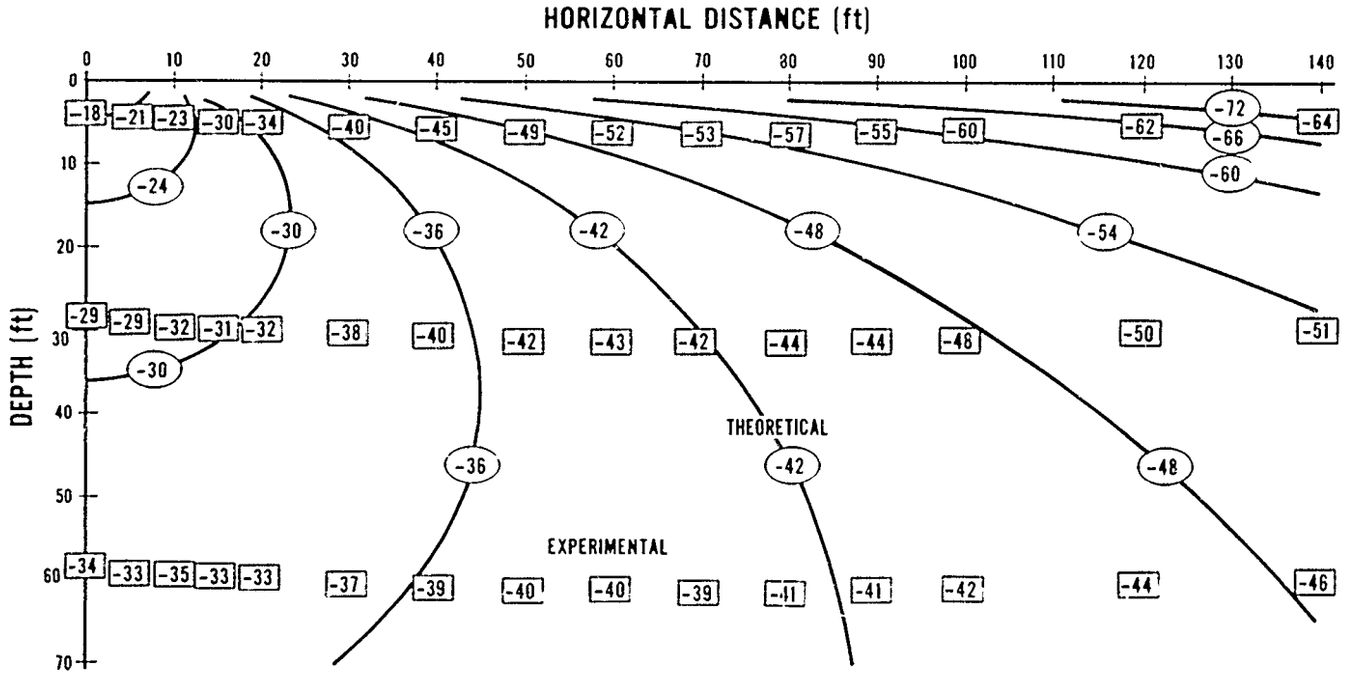


Figure 5-1. Comparison Between Ray Theory Predictions and Experimental Measurements of Underwater Sound Field Due to Airborne Point Source at Height of 30 feet

## REFERENCES

1. Hudimac, "Ray Theory for the Sound Intensity in Water Due to a Point Source Above It", Journal of the Acoustical Society of America (JASA) 29, 916 (1957).

2. Horton, Fundamentals of Sonar, U.S. Naval Institute (1957), pages 86 - 88, 109 - 110, and 117 - 120.

3. Brekhovskikh, Waves in Layered Media, Academic Press, New York (1960), p. 15 - 25.

4. Weinstein and Henney, "Wave Solution for Air-to-Water Sound Transmission", JASA 37, 899 (1964).

5. Young, "Sound Pressure in Water from Source in Air", JASA 50, 1392 (1971).

6. Waters and Glass, "Penetration of Sonic Boom Energy into the Ocean: An Experimental Simulation", Hydrospace Research Corporation Technical Report No. 288 (June 1970).

# APPENDIX A

## LISTINGS ØF CØMPUTER PRØGRAMS FØR DETERMINATIØN ØF UNDERWATER SØUND FIELDS DUE TØ AIRBØRNE PØINT SØURCES USING ACØUSTIC RAY THEØRY

PRØGRAMS LISTED:

/USF/
/AA/
/APLØT/
/ADDAMB/
/LPLØT/
/CØN/
/CPLØT/

PRØGRAMS ARE WRITTEN IN "SUPER BASIC" LANGUAGE FØR USE ØN "TYMSHARE" TIME-SHARING CØMPUTER

PRØGRAM /USF/

```
1000 PRINT "THIS IS PRØGRAM /USF/, FØR CØMPUTING THE UNDERWATER SØUND"
1010 PRINT "  FIELDS ASSØCIATED WITH AIRBØRNE SØUND SØURCES"
1020 PRINT
1030 PRINT "DATE AND TIME: ": DATE
1040 PRINT
1050 PRINT
1060 VAR = ZERØ
1070 G$ = TIME /60
1080 DIM L$(0:60), F$(0:60), P$(1:10,0:60), T$(1:10,0:60)
1090 INTEGER P1, R1, H1, D1, U, Y, S1, P0, K9
1100 V1 = 1085
1110 V2 = 4750
1120 R1 = 1.29
1130 R2 = 1025
1140 K1 = V2 / V1
1150 Z1 = (V1*R1) / (V2*R2)
1160 K2 = K1↑2
1170 K4 = K2↑2
1180 PRINT "WHAT IS SØURCE PRESSURE LEVEL, P1, IN DB//UBAR AT R1":
1190 INPUT P1
1200 PRINT
1210 PRINT "WHAT IS REFERENCE DISTANCE, R1, IN FEET":
1220 INPUT R1
1230 PRINT
1240 PRINT "WHAT IS HEIGHT, H1, ØF SØURCE ABØVE WATER, IN FEET":
1250 INPUT H1
1260 PRINT
1270 PRINT "WHAT IS ØFFSET DISTANCE, D1, FRØM SØURCE TØ VERTICAL AXIS"
1280 PRINT "  THRØUGH RECEIVER AT CLØSEST PØINT ØF APPRØACH, IN FEET":
1290 INPUT D1
1300 Q1 = K2 + 1
1310 Q2 = K2 + 2
1320 Q3 = 2 * K2 + 1
1330 Q4 = K4 + 4 * K2 + 1
1340 Q5 = 2 * K2
1350 Q6 = 2 * Q3
1360 Q7 = Q5 * Q2
1370 PRINT
1380 PRINT "WHAT IS GRID INCREMENT, U, IN FEET":
1390 INPUT U
```

```
1400 PRINT
1410 PRINT "WHAT IS MAXIMUM DISTANCE, Y, IN FEET":
1420 INPUT Y
1430 PRINT
1440 J9 = Y / U
1450 FØR J = 0 TØ J9
1460 D2 = J * U
1470 IF D1 = 0 AND D2 = 0 THEN F$(J) = 0
1480 IF D1 = 0 AND D2 > 0 THEN F$(J) = 90
1490 IF D1 > 0 AND D2 > 0 THEN F$(J) = (180/PI) * ATAN( D2/D1 )
1500 L$(J) = SQRT( D1↑2 + D2↑2 )
1510 IF L$(J) = 0 THEN L$(J) = 1E-6
1520 NEXT J
1530 P8 = 10 ↑ (P1/20)
1540 FØR I = 1 TØ 10
1550 H2 = I * U
1560 PRINT
1570 PRINT "
DEPTH, H2, ØF RECEIVER, IN FEET, = ":
1580 PRINT IN IMAGE "%%%%": H2
1590 PRINT
1600 PRINT "
  L2        PH2        TH1        TH2       PR      K"
1610 PRINT "
 (FT)      (DEG)      (DEG)      (DEG)     (DB)   (INT)"
1620 G1 = H1 ↑ 2
1630 G2 = H2 ↑ 2
1640 G3 = G1 ↑ 2
1650 G4 = G2 ↑ 2
1660 G9 = G1 * G2
1670 X = 0
1680 FØR J = 0 TØ J9
1690 K = 0
1700 M2 = (L$(J)) ↑ 2
1710 M4 = M2 ↑ 2
1720 M7 = M2 * G1
1730 M8 = M2 * G2
1740 A4 = K4 * ( (M2+G1+G2)↑2 - 4*G9 )
1750 A3 = -2 * K2 * ( Q1*(M4-G9) + G3 + K2*G4 + Q2*M7 + Q3*M8 )
1760 A2 = Q4*M4 + G3 + K4*G4 + Q6*M7 + Q7*M8 - Q5*G9
1770 A1 = -2 * ( Q1*M4 + M7 + K2*M8 )
1780 B4 = 4 * A4
1790 B3 = 3 * A3
1800 B2 = 2 * A2
1810 X2 = X ↑ 2
1820 X3 = X2 * X
1830 X4 = X3 * X
```

```
1840 F = A4*X4 + A3*X3 + A2*X2 + A1*X + M4
1850 G = B4*X3 + B3*X2 + B2*X + A1
1860 E = F / G
1870 X = X - E
1880 K = K + 1
1890 IF K > 50 THEN 1910
1900 IF ABS(E) > 0.000001*X THEN 1810
1910 T1 = ATAN( SQRT( X/(1-X) ) )
1920 S2 = (K1 * SIN(T1)) ↑ 2
1930 IF S2 >= 1 THEN S2 = 0.9999999999999
1940 T2 = ATAN( SQRT( S2/(1-S2) ) )
1950 C1 = COS(T1)
1960 B = COS(T2) / C1
1970 P7 = 2 * R1 * C1
1980 P2 = 1 + B*Z1
1990 A = K1 * H2 / B
2000 P3 = H1 + A
2010 P4 = H1 + A / (B↑2)
2020 P9 = ABS( P8*P7/(P2*SQRT(P3*P4)) )
2030 IF P9 < 1E-10 THEN P9 = 1E-10
2040 P$(I,J) = 20 * LOG10( P9 )
2050 T$(I,J) = (180/PI) * T2
2060 T1 = (180/PI) * T1
2070 S = "
%%%%%BB%%%%.%%%BB%%%%.%%%BB%%%%.%%%BB%%%%.%BB%%%B/"
2080 PRINT IN FORM S: L$(J), F$(J), T1, T$(I,J), P$(I,J), K
2090 NEXT J
2100 PRINT
2110 NEXT I
2120 OPEN /ADATA/, BINARY OUTPUT, 1
2130 OPEN /CDATA/, BINARY OUTPUT, 3
2140 WRITE ON 1: T$(I,J) FOR J = 0 TO J9 FOR I = 1 TO 10
2150 WRITE ON 3: P$(I,J) FOR J = 0 TO J9 FOR I = 1 TO 10
2160 CLOSE 1, 3
2170 K9 = 0
2180 OPEN /UYDATA/, BINARY OUTPUT, 9
2190 WRITE ON 9: P1, R1, H1, D1, U, Y, S1, P0, K9
2200 CLOSE 9
2210 PRINT
2220 PRINT
2230 PRINT "THIS COMPLETES THE OUTPUT OF DATA FROM PROGRAM /USF/."
2240 PRINT
2250 PRINT "OUTPUT FROM /USF/ IS STORED IN /ADATA/ AND /CDATA/."
2260 PRINT
2270 G2 = TIME/60
2280 INTEGER G3
2290 G3 = G2 - G$
2300 PRINT G3: " TOTAL ELAPSED SECONDS"
```

PRØGRAM /AA/

```
1000 PRINT "THIS IS PRØGRAM /AA/, FØR CØMPUTING THE ANGLE ØF"
1010 PRINT "  ARRIVAL ØF UNDERWATER SIGNAL RELATIVE TØ THE"
1020 PRINT "  HØRIZØNTAL AXIS ØF A SØNAR RECEIVER AT VARIØUS"
1030 PRINT "  HEADINGS AND AT VARIØUS DEPTHS"
1040 PRINT
1050 PRINT "DATE AND TIME: ": DATE
1060 PRINT
1070 PRINT
1080 VAR = ZERØ
1090 G1 = TIME/60
1100 DIM F$(-60:60)
1110 REAL T$(1:10,-60:60), A$(1:3,1:4,-60:60)
1120 INTEGER P1, R1, H1, D1, U, Y, S$, PØ, K9
1130 IF D1 = 0 THEN D1 = 1E-6
1140 ØPEN /UYDATA/, BINARY INPUT, 9
1150 INPUT FRØM 9: P1, R1, H1, D1, U, Y, S$, PØ, K9
1160 CLØSE 9
1170 I1 = 0
1180 J9 = Y / U
1190 FØR J = -J9 TØ J9
1200 D2 = J * U
1210 IF D1 = 0 AND D2 < 0 THEN F$(J) = -90
1220 IF D1 = 0 AND D2 = 0 THEN F$(J) = 0
1230 IF D1 = 0 AND D2 > 0 THEN F$(J) = 90
1240 IF D1 > 0 THEN F$(J) = (180/PI) * ATAN( D2/D1 )
1250 NEXT J
1260 ØPEN /ADATA/, BINARY INPUT, 1
1270 INPUT FRØM 1: T$(I,J) FØR J = 0 TØ J9 FØR I = 1 TØ 10
1280 CLØSE 1
1290 SØ = "'DEPTH ØF RECEIVER (FEET) ='%%%//"
1300 S1 = "'HEADING ØF RECEIVER (DEGREES) ='%%%//"
1310 S2 = "10(%%%.%B)/"
1320 S3 = "   %%%.%B /"
1330 FØR H2 = 200, 400, 800
1340 I1 = I1 + 1
1350 PRINT IN FØRM SØ: H2
1360 I = H2/U
1370 PRINT
1380 PRINT "
ANGLES, THETA(A), ØF SIGNAL ARRIVAL RELATIVE TØ HØRIZØNTAL"
```

```
1390 PRINT "
PERPENDICULAR BISECTØR ØF AXIS ØF RECEIVER (DEGREES):"
1400 FØR K = 1 TØ 4
1410 F2 = 30 * (K-1)
1420 FØR J1 = 1 TØ J9
1430 J = -J1
1440 T$(I,J) = T$(I,J1)
1450 NEXT J1
1460 FØR J = -J9 TØ J9
1470 A1 = (PI/180) * ( F2 - F$(J) )
1480 A2 = (PI/180) * T$(I,J)
1490 B1 = CØS(A1) * SIN(A2)
1500 B2 = SGN(B1)
1510 B3 = B1 ↑ 2
1520 A$(I1,K,J) = B2 * (180/PI) * ATAN( SQRT(B3/(1-B3) ) )
1530 NEXT J
1540 PRINT
1550 PRINT IN FØRM S1: F2
1560 PRINT IN FØRM S2: A$(I1,K,J) FØR J = -J9 TØ -1
1570 PRINT IN FØRM S3: A$(I1,K,0)
1580 PRINT IN FØRM S2: A$(I1,K,J) FØR J = 1 TØ J9
1590 PRINT
1600 NEXT K
1610 PRINT
1620 NEXT H2
1630 ØPEN /BDATA/, BINARY ØUTPUT, 2
1640 FØR I1 = 1 TØ 3
1650 WRITE ØN 2: A$(I1,K,J) FØR J = -J9 TØ J9 FØR K = 1 TØ 4
1660 NEXT I1
1670 CLØSE 2
1680 PRINT
1690 PRINT
1700 PRINT "THIS CØMPLETES THE ØUTPUT ØF DATA FRØM PRØGRAM /AA/."
1710 PRINT
1720 PRINT "ØUTPUT FRØM /AA/ IS STØRED IN /BDATA/."
1730 PRINT
1740 G2 = TIME/60
1750 INTEGER G3
1760 G3 = G2 - G1
1770 PRINT G3: " TØTAL ELAPSED SECØNDS"
```

PRØGRAM /APLØT/

```
1000 PRINT "THIS IS PRØGRAM /APLØT/, FØR PLØTTING TIME HISTØRIES"
1010 PRINT "  ØF ANGLES ØF ARRIVAL AT SØNAR RECEIVER"
1020 PRINT
1030 PRINT "DATE AND TIME: ": DATE
1040 PRINT
1050 PRINT
1060 VAR = ZERØ
1070 G1 = TIME/60
1080 REAL A$(1:3,1:4,-60:60)
1090 INTEGER P1, R1, H1, D1, U, Y, S1, PØ, K9
1100 ØPEN /UYDATA/, BINARY INPUT, 9
1110 INPUT FRØM 9: P1, R1, H1, D1, U, Y, S1, PØ, K9
1120 CLØSE 9
1130 J9 = Y / U
1140 PRINT "WHAT IS AIRCRAFT SPEED, S1, IN KNØTS":
1150 INPUT S1
1160 PRINT
1170 TØ = (3600/6076) * (U/S1)
1180 T1 = 20*TØ
1190 ØPEN /BDATA/, BINARY INPUT, 2
1200 ØPEN /APDATA/, ØUTPUT, 8
1210 FØR I1 = 1 TØ 3
1220 XØ = 500 + (I1-1)*1000
1230 YØ = 500
1240 INPUT FRØM 2: A$(I1,K,J) FØR J = -J9 TØ J9 FØR K = 1 TØ 4
1250 Ø = "%%%%%%B%%%%B%/"
1260 FØR K = 1 TØ 4
1270 Z = 0
1280 FØR J = -J9 TØ J9
1290 X = XØ + J*T1
1300 Y = YØ + 2.5*A$(I1,K,J)
1310 WRITE ØN 8 IN FØRM Ø: X, Y, Z
1320 Z = 1
1330 NEXT J
1340 NEXT K
1350 NEXT I1
1360 X = 3500
1370 Y = 0
1380 Z = 0
1390 WRITE ØN 8 IN FØRM Ø: X, Y, Z
```

```
1400 CLØSE 8
1410 CLØSE 2
1420 PRINT
1430 PRINT
1440 PRINT "THIS CØMPLETES THE ØUTPUT ØF DATA FRØM PRØGRAM /APLØT/."
1450 PRINT
1460 PRINT "ØUTPUT FRØM /APLØT/ IS STØRED IN /APDATA/,"
1470 PRINT "  READY FØR PUNCHING ØUT ØN PAPER TAPE."
1480 PRINT
1490 G2 = TIME/60
1500 INTEGER G3
1510 G3 = G2 - G1
1520 PRINT G3; " TØTAL ELAPSED SECØNDS"
```

PRØGRAM /ADDAMB/

```
1000 PRINT "THIS IS PRØGRAM /ADDAMB/, FØR CØMPUTING ADDED EFFECTS ØF"
1010 PRINT "  AMBIENT NØISE ØN TØTAL UNDERWATER SØUND FIELD"
1020 PRINT
1030 PRINT "DATE AND TIME: ": DATE
1040 PRINT
1050 PRINT
1060 VAR = ZERØ
1070 G1 = TIME/60
1080 REAL P$(1:10,0:60)
1090 INTEGER P1, R1, H1, D1, U, Y, S1, PØ, K9
1100 ØPEN /UYDATA/, BINARY INPUT, 9
1110 INPUT FRØM 9: P1, R1, H1, D1, U, Y, S1, PØ, K9
1120 CLØSE 9
1130 J9 = Y / U
1140 PRINT "WHAT IS AMBIENT SØUND PRESSURE LEVEL, PØ, IN DB//UBAR":
1150 INPUT PØ
1160 PRINT
1170 ØPEN /UYDATA/, BINARY ØUTPUT, 9
1180 WRITE ØN 9: P1, R1, H1, D1, U, Y, S1, PØ, K9
1190 CLØSE 9
1200 P8 = 10↑(PØ/10)
1210 ØPEN /CDATA/, BINARY INPUT, 3
1220 INPUT FRØM 3: P$(I,J) FØR J = 0 TØ J9 FØR I = 1 TØ 10
1230 CLØSE 3
1240 FØR I = 1 TØ 10
1250 FØR J = 0 TØ J9
1260 P7 = 10↑(P$(I,J)/10)
1270 P$(I,J) = 10*LØG10(P7+P8)
1280 NEXT J
1290 NEXT I
1300 ØPEN /FDATA/, BINARY ØUTPUT, 6
1310 WRITE ØN 6: P$(I,J) FØR J = 0 TØ J9 FØR I = 1 TØ 10
1320 CLØSE 6
1330 PRINT
1340 PRINT
1350 PRINT "THIS CØMPLETES THE ØUTPUT ØF DATA FRØM PRØGRAM /ADDAMB/."
1360 PRINT
1370 PRINT "ØUTPUT FRØM /ADDAMB/ IS STØRED IN /FDATA/."
1380 PRINT
1390 G2 = TIME/60
1400 INTEGER G3
1410 G3 = G2 - G1
1420 PRINT G3: " TØTAL ELAPSED SECØNDS"
```

PRØGRAM /LPLØT/

```
1000 PRINT "THIS IS PRØGRAM /LPLØT/, FØR PLØTTING TIME HISTØRIES"
1010 PRINT "  ØF USF SPLS AT SØNAR RECEIVERS AT VARIØUS DEPTHS"
1020 PRINT
1030 PRINT "DATE AND TIME: ": DATE
1040 PRINT
1050 PRINT
1060 VAR = ZERØ
1070 G1 = TIME/60
1080 REAL P$(1:10,0:60)
1090 INTEGER P1, R1, H1, D1, U, Y, S1, PO, K9
1100 ØPEN /UYDATA/, BINARY INPUT, 9
1110 INPUT FRØM 9: P1, R1, H1, D1, U, Y, S1, PO, K9
1120 CLØSE 9
1130 PRINT "WHAT IS AIRCRAFT SPEED, S1, IN KNØTS":
1140 INPUT S1
1150 PRINT
1160 J9 = Y / U
1170 TO = (3600/6076) * (U/S1)
1180 T1 = 20*TO
1190 PRINT "AMBIENT SØUND PRESSURE LEVEL IS ": PO: " DB//UBAR"
1200 PRINT
1210 ØPEN /FDATA/, BINARY INPUT, 6
1220 INPUT FRØM 6: P$(I,J) FØR J = 0 TØ J9 FØR I = 1 TØ 10
1230 CLØSE 6
1240 ØPEN /LPDATA/, ØUTPUT, 8
1250 Ø = "%%%%%%B%%%%B%/"
1260 XO = 500
1270 YO = 500
1280 FØR I = 1, 2, 4, 8
1290 Z = 0
1300 FØR J = -J9 TØ J9
1310 X = XO + J*T1
1320 Y = YO + 5*P$(I,ABS(J))
1330 WRITE ØN 8 IN FØRM Ø: X, Y, Z
1340 Z = 1
1350 NEXT J
1360 NEXT I
1370 Y = YO + 5*PO
1380 FØR J = -J9 TØ J9 BY 6
1390 X = XO + J*T1
```

```
1400 Z = 0
1410 WRITE ØN 8 IN FØRM 0: X, Y, Z
1420 X = X + 4*T1
1430 Z = 1
1440 WRITE ØN 8 IN FØRM 0: X, Y, Z
1450 NEXT J
1460 X = 1500
1470 Y = 0
1480 Z = 0
1490 WRITE ØN 8 IN FØRM 0: X, Y, Z
1500 CLØSE 8
1510 PRINT
1520 PRINT
1530 PRINT "THIS CØMPLETES THE ØUTPUT ØF DATA FRØM PRØGRAM /LPLØT/."
1540 PRINT
1550 PRINT "ØUTPUT FRØM /LPLØT/ IS STØRED ØN /LPDATA/,"
1560 PRINT "  READY FØR PUNCHING ØUT ØN PAPER TAPE."
1570 PRINT
1580 G2 = TIME/60
1590 INTEGER G3
1600 G3 = G2 - G1
1610 PRINT G3; " TØTAL ELAPSED SECØNDS"
```

PRØGRAM /CØN/

```
1000 PRINT "THIS IS PRØGRAM /CØN/, FØR CØMPUTING EQUIPRESSURE CØNTØURS"
1010 PRINT "  ASSØCIATED WITH UNDERWATER SØUND FIELD INCLUDING AMBIENT"
1020 PRINT
1030 PRINT "DATE AND TIME: ": DATE
1040 PRINT
1050 PRINT
1060 VAR = ZERØ
1070 G1 = TIME/60
1080 INTEGER P1, R1, H1, D1, U, Y, S$, P0, K9, Y2
1090 INTEGER L$(1:50)
1100 REAL P$(1:10,0:60), E$(1:50)
1110 REAL Y$(1:200), Z$(1:200)
1120 ØPEN /UYDATA/, BINARY INPUT, 9
1130 INPUT FRØM 9: P1, R1, H1, D1, U, Y, S$, P0, K9
1140 CLØSE 9
1150 J9 = Y / U
1160 ØPEN /FDATA/, BINARY INPUT, 6
1170 INPUT FRØM 6: P$(I,J) FØR J = 0 TØ J9 FØR I = 1 TØ 10
1180 CLØSE 6
1190 PRINT "WHAT IS MAXIMUM DISTANCE, Y2, TØ WHICH UNDERWATER"
1200 PRINT "  EQUIPRESSURE CØNTØURS ARE TØ BE CØMPUTED, IN FEET":
1210 INPUT Y2
1220 PRINT
1230 J9 = Y2/U
1240 PRINT "THE MAXIMUM UNDERWATER SPL IS ": INT(P$(1,0)): " DB//UBAR"
1250 PRINT
1260 PRINT "THE MINIMUM UNDERWATER SPL IS ": INT(P$(1,J9)): " DB//UBAR"
1270 PRINT
1280 PRINT "WHAT IS DESIRED CØNTØUR INTERVAL, C2, IN THE"
1290 PRINT "  SPECIFIED UNDERWATER REGIØN, IN DB":
1300 INPUT C2
1310 PRINT
1320 ØPEN /EDATA/, BINARY ØUTPUT, 5
1330 DEF FNA(P) = 10 ↑ (P/20)
1340 K1 = INT( P$(1,0) / C2 )
1350 K2 = INT( P$(1,J9) / C2 )
1360 K9 = K1 - K2
1370 PRINT "THERE ARE ": K9: " EQUIPRESSURE CØNTØURS IN THE"
1380 PRINT "  SPECIFIED UNDERWATER REGIØN"
1390 PRINT
```

```
1400 FØR K = 1 TØ K9
1410 L$(K) = 0
1420 E$(K) = (K1+1-K) * C2
1430 NEXT K
1440 FØR K = 1 TØ K9
1450 FØR J = 0 TØ J9
1460 FØR I = 1 TØ 9
1470 F2 = P$(I,J) - P$(I+1,J)
1480 F = ( P$(I,J) - E$(K) ) / F2
1490 IF F < 0 ØR F >= 1 THEN 1570
1500 L$(K) = L$(K) + 1
1510 L = L$(K)
1520 F1 = FNA( P$(I,J) ) - FNA( E$(K) )
1530 F2 = FNA( P$(I,J) ) - FNA( P$(I+1,J) )
1540 F = F1/F2
1550 Y$(L) = J * U
1560 Z$(L) = ( I+F ) * U
1570 NEXT I
1580 NEXT J
1590 FØR I = 1 TØ 10
1600 FØR J = 0 TØ (J9-1)
1610 F2 = P$(I,J) - P$(I,J+1)
1620 F = ( P$(I,J) - E$(K) ) / F2
1630 IF F < 0 ØR F >= 1 THEN 1710
1640 L$(K) = L$(K) + 1
1650 L = L$(K)
1660 F1 = FNA( P$(I,J) ) - FNA( E$(K) )
1670 F2 = FNA( P$(I,J) ) - FNA( P$(I,J+1) )
1680 F = F1/F2
1690 Y$(L) = ( J+F ) * U
1700 Z$(L) = I * U
1710 NEXT J
1720 NEXT I
1730 FØR I = 1 TØ 9
1740 FØR J = 0 TØ (J9-1)
1750 F2 = P$(I,J) - P$(I+1,J+1)
1760 F = ( P$(I,J) - E$(K) ) / F2
1770 IF F < 0 ØR F >= 1 THEN 1850
1780 L$(K) = L$(K) + 1
1790 L = L$(K)
1800 F1 = FNA( P$(I,J) ) - FNA( E$(K) )
1810 F2 = FNA( P$(I,J) ) - FNA( P$(I+1,J+1) )
1820 F = F1/F2
1830 Y$(L) = ( J+F ) * U
1840 Z$(L) = ( I+F ) * U
1850 NEXT J
1860 NEXT I
```

```
1870 FØR I = 1 TØ 9
1880 FØR J = 1 TØ J9
1890 F2 = P$(I,J) - P$(I+1,J-1)
1900 F = ( P$(I,J) - E$(K) ) / F2
1910 IF F < 0 ØR F >= 1 THEN 1990
1920 L$(K) = L$(K) + 1
1930 L = L$(K)
1940 F1 = FNA( P$(I,J) ) - FNA( E$(K) )
1950 F2 = FNA( P$(I,J) ) - FNA( P$(I+1,J-1) )
1960 F = F1/F2
1970 Y$(L) = ( J-F ) * U
1980 Z$(L) = ( I+F ) * U
1990 NEXT J
2000 NEXT I
2010 S1 = "%%%%B"
2020 PRINT IN FØRM S1: E$(K)
2030 PRINT "DB CØNTØUR PØINTS"
2040 FØR L1 = 1 TØ L$(K)
2050 Z9 = -1
2060 FØR L = 1 TØ L$(K)
2070 IF Z$(L) < Z9 THEN 2100
2080 Z9 = Z$(L)
2090 L9 = L
2100 NEXT L
2110 S2 = "%%%%%.%%BB%%%%%.%%/"
2120 PRINT IN FØRM S2: Y$(L9), Z$(L9)
2130 WRITE ØN 5: Y$(L9), Z$(L9)
2140 Z$(L9) = -1
2150 NEXT L1
2160 PRINT
2170 NEXT K
2180 ØPEN /DDATA/, BINARY ØUTPUT, 4
2190 WRITE ØN 4: L$(K) FØR K = 1 TØ K9
2200 CLØSE 4
2210 CLØSE 5
2220 ØPEN /UYDATA/, BINARY ØUTPUT, 9
2230 WRITE ØN 9: P1, R1, H1, D1, U, Y, S$, PO, K9, Y2
2240 CLØSE 9
2250 PRINT
2260 PRINT
2270 PRINT "THIS CØMPLETES THE ØUTPUT ØF DATA FRØM PRØGRAM /CØN/."
2280 PRINT
2290 PRINT "ØUTPUT FRØM /CØN/ IS STØRED IN /DDATA/ AND /EDATA/."
2300 PRINT
2310 G2 = TIME/60
2320 INTEGER G3
2330 G3 = G2 - G1
2340 PRINT G3: " TØTAL ELAPSED SECØNDS"
```

PRØGRAM /CPLØT/

```
1000 PRINT "THIS IS PRØGRAM /CPLØT/, FØR PLØTTING EQUIPRESSURE"
1010 PRINT "  CØNTØURS FØR USF SPLS INCLUDING AMBIENT EFFECTS"
1020 PRINT
1030 PRINT "DATE AND TIME: ": DATE
1040 PRINT
1050 PRINT
1060 VAR = ZERØ
1070 G1 = TIME/60
1080 INTEGER L$(1:50)
1090 REAL Y$(1:200), Z$(1:200)
1100 INTEGER P1, R1, H1, D1, U, Y, S1, PO, K9, Y2
1110 INTEGER E
1120 ØPEN /UYDATA/, BINARY INPUT, 9
1130 INPUT FRØM 9: P1, R1, H1, D1, U, Y, S1, PO, K9, Y2
1140 CLØSE 9
1150 J9 = Y2 / U
1160 C = 50/U
1170 ØPEN /DDATA/, BINARY INPUT, 4
1180 INPUT FRØM 4: L$(K) FØR K = 1 TØ K9
1190 CLØSE 4
1200 ØPEN /EDATA/, BINARY INPUT, 5
1210 ØPEN /CPDATA/, ØUTPUT, 8
1220 Ø = "%%%%%%B%%%%B%/"
1230 X1 = 0
1240 Y1 = 0
1250 XO = 0
1260 YO = 600
1270 X = XO
1280 Y = YO
1290 Z = 0
1300 WRITE ØN 8 IN FØRM Ø: X, Y, Z
1310 X = XO + C*Y2
1320 Z = 1
1330 WRITE ØN 8 IN FØRM Ø: X, Y, Z
1340 FØR K = 1 TØ K9
1350 Z = 0
1360 FØR L = 1 TØ L$(K)
1370 INPUT FRØM 5: Y$(L), Z$(L)
1380 NEXT L
```

```
1390 FØR L = 1 TØ L$(K)
1400 X = X0 + C*Y$(L)
1410 Y = Y0 - C*Z$(L)
1420 IF ABS(X-X1) < 50*C AND ABS(Y-Y1) < 20*C THEN 1470
1430 X1 = X
1440 Y1 = Y
1450 WRITE ØN 8 IN FØRM 0: X, Y, Z
1460 Z = 1
1470 NEXT L
1480 NEXT K
1490 IF H1>=4*U THEN P9 = P1 - 20*LØG( (H1-4*U)/R1 )
1500 IF H1<4*U THEN P9 = P1 - 30
1510 P8 = P1 - 20*L0G10( (SQRT(H1↑2+(J9*U)↑2))/R1 )
1520 PRINT "THE MAXIMUM SPL IN THE ATMØSPHERIC REGIØN"
1530 PRINT "  ØF INTEREST IS ": INT(P9): " DB//UBAR"
1540 PRINT
1550 PRINT "THE MINIMUM SPL IN THE  .10SPHERIC REGIØN"
1560 PRINT "  ØF INTEREST IS ": INT(P8): " DB//UBAR"
1570 PRINT
1580 PRINT "WHAT IS DESIRED CØNTØUR INTERVAL, C1, IN AIR JUST ABØVE"
1590 PRINT "  SURFACE ØF SPECIFIED UNDERWATER REGIØN, IN DB":
1600 INPUT C1
1610 PRINT
1620 K1 = INT( P9/C1 )
1630 K2 = INT( P8/C1 )
1640 K8 = K1 - K2
1650 FØR K = 1 TØ K8
1660 E = (K1+1-K) * C1
1670 PRINT "CØNTØUR ": K: " IN AIR IS ": E: " DB//UBAR"
1680 R = C * R1 * 10↑( (P1-E)/20 )
1690 Z = 0
1700 FØR L = 0 TØ Y2 BY 10
1710 X = X0 + C*L
1720 IF X > R THEN 1790
1730 Y = Y0 + C*H1 - SQRT(R↑2-X↑2)
1740 IF Y <= Y0 THEN 1780
1750 WRITE ØN 8 IN FØRM 0: X, Y, Z
1760 IF Y > Y0 + 200 THEN 1790
1770 Z = 1
1780 NEXT L
1790 NEXT K
1800 X = X0 + C*Y2 + 500
1810 Y = 0
1820 Z = 0
1830 WRITE ØN 8 IN FØRM 0: X, Y, Z
1840 CLØSE 8
1850 CLØSE 5
1860 PRINT
1870 PRINT
```

```
1880 PRINT "THIS CØMPLETES THE ØUTPUT ØF DATA FRØM PRØGRAM /CPLØT/."
1890 PRINT
1900 PRINT "ØUTPUT FRØM /CPLØT/ IS STØRED IN /CPDATA/,"
1910 PRINT "  READY FØR PUNCHING ØUT ØN PAPER TAPE."
1920 PRINT
1930 G2 = TIME/60
1940 INTEGER G3
1950 G3 = G2 - G1
1960 PRINT G3: " TØTAL ELAPSED SECØNDS"
```

# DISTRIBUTION LIST

| | No. of Copies |
|---|---|
| Office of Naval Research (Code 468)<br>Department of the Navy<br>Arlington, Virginia 22217 | 2 |
| Director, Naval Research Laboratory<br>Technical Information Division<br>Department of the Navy<br>Washington, D. C. 20390 | 3 |
| Director, Advanced Research Projects Agency<br>Technical Library, The Pentagon<br>Washington, D. C. 20301 | 3 |
| Defense Documentation Center<br>Cameron Station<br>Alexandria, Virginia 22314 | 12 |
| Commanding Officer<br>Office of Naval Research Branch Office<br>219 S. Dearborn Street<br>Chicago, Illinois 60604 | 1 |
| Commanding Officer<br>Office of Naval Research Branch Office<br>1030 East Green Street<br>Pasadena, California 91101 | 1 |
| Commanding Officer<br>Office of Naval Research Branch Office<br>495 Summer Street<br>Boston, Massachusetts 02210 | 1 |
| San Francisco Area Office<br>Office of Naval Research<br>1076 Mission Street<br>San Francisco, California 94109 | 1 |
| New York Area Office<br>Office of Naval Research<br>207 W. 24th Street<br>New York, New York 10011 | 1 |

DISTRIBUTION LIST (Contd.)

| | No. of Copies |
|---|---|
| Director<br>Naval Research Laboratory<br>Library, Code 2029 (ONRL)<br>Washington, D. C. 20390 | 2 |
| Commander<br>Naval Ordnance Laboratory<br>Acoustics Division<br>White Oak, Silver Spring, Maryland 20910 | 1 |
| Commander<br>Navy Undersea Research & Development Center<br>Technical Library<br>San Diego, California 92152 | 1 |
| Officer-in-Charge<br>Technical Library<br>Naval Underwater Systems Center<br>Newport, Rhode Island 02840 | 1 |
| Commanding Officer<br>Technical Library<br>Naval Underwater Systems Center<br>Fort Trumbull, New London, Connecticut 06321 | 1 |
| Naval Ship Research and Development Center<br>Central Library<br>Washington, D. C. 20034 | 1 |
| Commanding Officer<br>Naval Air Development Center<br>Johnsville, Warminster, Pennsylvania 18974 | 1 |
| Commanding Officer<br>Navy Mine Defense Laboratory<br>Panama City, Florida 32402 | 1 |
| Naval Research Laboratory<br>Underwater Sound Reference Division<br>Technical Library<br>P. O. Box 8337<br>Orlando, Florida 32806 | 1 |
| Naval Weapons Center<br>Technical Library<br>China Lake, California 93555 | 1 |

DISTRIBUTION LIST (Contd.)

| | No. of Copies |
|---|---|
| Naval Undersea Warfare Center<br>Technical Library<br>3202 E. Foothill Boulevard<br>Pasadena, California 91107 | 1 |
| Office of the Director of Defense<br>Research and Engineering<br>Information Office Library Branch<br>The Pentagon<br>Washington, D. C. 20301 | 1 |
| U. S. Army Research Office<br>Box CM, Duke Station<br>Durham, North Carolina 27706 | 1 |
| Air Force Office of Scientific Research<br>Department of the Air Force<br>Washington, D. C. 20333 | 1 |
| Air Force Avionics Laboratory<br>Air Force Systems Command<br>Technical Library<br>Wright-Patterson Air Force Base<br>Dayton, Ohio 45433 | 1 |
| Naval Postgraduate School<br>Technical Library<br>Monterey, California 93940 | 1 |
| Naval Academy<br>Technical Library<br>Annapolis, Maryland 21401 | 1 |
| Research & Technology Directorate<br>Naval Electronics Systems Command<br>Department of the Navy<br>Washington, D. C. 20360 | 1 |
| RDT&E Planning Division<br>Naval Ship Systems Command<br>Department of the Navy<br>Washington, D. C. 20360 | 1 |

DISTRIBUTION LIST (Contd.)

| | No. of Copies |
|---|---|
| Research and Technology<br>Naval Air Systems Command<br>Department of the Navy<br>Washington, D. C. 20360 | 1 |
| Research and Technology Directorate<br>Naval Ordnance Systems Command<br>Department of the Navy<br>Washington, D. C. 20360 | 1 |
| Office of Naval Research<br>Code 461<br>Department of the Navy<br>Arlington, Virginia 22217 | 1 |
| Hydrospace Research Corporation<br>2150 Fields Road<br>Rockville, Maryland 20850 | 10 |
| General Electric Company<br>Mr. R. J. Twardzik<br>Court Street, Plant No. 9<br>Syracuse, New York 13201 | 1 |
| Mr. R. J. Urick<br>Research Acoustics Division<br>U. S. Naval Ordnance Laboratory<br>Silver Spring, Maryland 20910 | 1 |
| Mr. I. Sochard<br>U. S. Naval Ordnance Laboratory<br>Silver Spring, Maryland 20910 | 1 |
| Mr. R. W. Young<br>Naval Undersea Research & Development Center<br>San Diego, California 92132 | 1 |
| Dr. A. A. Hudimac<br>Scientific Research Associates, Inc.<br>12100 Devilwood Drive<br>Potomac, Maryland 20854 | 1 |

DISTRIBUTION LIST (Contd.)

| | No. of Copies |
|---|---|
| Lt. D. H. Bennet<br>U. S. Naval Ship Systems Command<br>Department of the Navy<br>Washington, D. C. 20360 | 1 |
| Dr. M. S. Weinstein<br>Underwater Systems, Inc.<br>8121 Georgia Avenue<br>Silver Spring, Maryland 20910 | 1 |
| Mr. Glenn Elmer<br>U. S. Naval Ship Research & Development Center<br>Washington, D. C. 20034 | 1 |
| Mr. D. A. Hilton<br>National Aeronautics & Space Administration<br>Langley Research Center<br>Hampton, Virginia 23365 | 1 |
| Mr. John Bellino<br>U. S. Naval Air Systems Command<br>Department of the Navy<br>Washington, D. C. 20360 | 1 |
| Dr. D. Bordelon<br>Naval Underwater Systems Center<br>Newport, Rhode Island 02840 | 1 |
| Mr. J. Conrad<br>U. S. Naval Scientific & Technical Intelligence Center<br>4301 Suitland Road<br>Suitland, Maryland | 1 |
| Mr. L. Freeman<br>Naval Underwater Systems Center<br>New London, Connecticut 06320 | 1 |
| Dr. J. Macaluso<br>Ordnance Research Laboratory<br>Penn State University<br>University Park, Pennsylvania 16801 | 1 |

DISTRIBUTION LIST (Contd.)

| | No. of Copies |
|---|---|
| Dr. J. C. Munson<br>U. S. Naval Research Laboratory<br>Washington, D. C. 20390 | 1 |
| Dr. H. Medwin<br>U. S. Navy Postgraduate School<br>Monterey, California 93940 | 1 |
| Mr. E. Wynnuzzi<br>U. S. Naval Air Development Center<br>Johnsville, Pennsylvania 18974 | 1 |
| Mr. Donald Rothacker<br>Riverside Research Institute<br>80 West End Avenue<br>New York, New York 10023 | 1 |
| Mr. R. Uranicar (Code 370E)<br>Naval Air Systems Command<br>Department of the Navy<br>Washington, D. C. 20360 | 1 |
| Sonar Directorate (Ships 901)<br>Naval Ship Systems Command<br>Department of the Navy<br>Washington, D. C. 20360 | 1 |
| Acoustic Warfare Project (PMS-394)<br>Naval Ship Systems Command<br>Department of the Navy<br>Washington, D. C. 20360 | 1 |

UNCLASSIFIED

Security Classification

**DOCUMENT CONTROL DATA - R & D**

*(Security classification of title, body of abstract and indexing annotation must be entered when the overall report is classified)*

| 1 ORIGINATING ACTIVITY (Corporate author) | 2a. REPORT SECURITY CLASSIFICATION |
|---|---|
| Hydrospace Research Corporation<br>2150 Fields Road<br>Rockville, Maryland 20850 | Unclassified |
| | 2b. GROUP<br>NA |

3 REPORT TITLE

COMPUTER PROGRAMS FOR UNDERWATER SOUND FIELDS DUE TO AIRBORNE SOURCES

4 DESCRIPTIVE NOTES (Type of report and inclusive dates)

Final - Technical Note

5 AUTHOR(S) (First name, middle initial, last name)

John F. Waters

| 6 REPORT DATE | 7a. TOTAL NO. OF PAGES | 7b. NO. OF REFS |
|---|---|---|
| January 1972 | 74 | 6 |

| 8a CONTRACT OR GRANT NO | 9a. ORIGINATOR'S REPORT NUMBER(S) |
|---|---|
| N00014-70-C-0301<br>b. PROJECT NO<br>c.<br>d. | Technical Note No. 144<br>9b. OTHER REPORT NO(S) (Any other numbers that may be assigned this report)<br>NONE |

10 DISTRIBUTION STATEMENT

NA

| 11 SUPPLEMENTARY NOTES | 12. SPONSORING MILITARY ACTIVITY |
|---|---|
| NA | Office of Naval Research<br>Code 468<br>Arlington, Virginia 22217 |

13 ABSTRACT

An aircraft flying over water produces a significant underwater sound field in the water directly beneath it. Acoustic ray theory can be used to obtain a useful approximate description of the underwater sound field in terms of sound pressure levels. Details of the theory are presented. Computer programs which implement the theory are documented. The results include time histories of acoustic signal angles of arrival at the underwater receiver; time histories of sound pressure levels received at various depths; and equipressure contour descriptions of the underwater sound field.

DD FORM 1 NOV 68 1473 REPLACES DD FORM 1473, 1 JAN 64, WHICH IS OBSOLETE FOR ARMY USE.

UNCLASSIFIED

Security Classification

| 14 KEY WORDS | LINK A | | LINK B | | LINK C | |
|---|---|---|---|---|---|---|
| | ROLE | WT | ROLE | WT | ROLE | WT |
| Aircraft Noise | | | | | | |
| Underwater Sound Field | | | | | | |
| Sound Transmission from Air into Water | | | | | | |